

On the origin of neural scaling laws: from random graphs to natural language

Maissam Barkeshli^{1,2,*}, Alberto Alfarano^{3,†,*}, Andrey Gromov¹

¹Meta Superintelligence Labs, FAIR, ²Department of Physics, University of Maryland, College Park and Joint Quantum Institute, ³Axiom Math

*Equal contribution, [†]Work done at Meta

Scaling laws have played a major role in the modern AI revolution, providing practitioners predictive power over how the model performance will improve with increasing data, compute, and number of model parameters. This has spurred an intense interest in the origin of neural scaling laws, with a common suggestion being that they arise from power law structure already present in the data. In this paper we study scaling laws for transformers trained to predict random walks (bigrams) on graphs with tunable complexity. We demonstrate that this simplified setting already gives rise to neural scaling laws even in the absence of power law structure in the data correlations. We further consider dialing down the complexity of natural language systematically, by training on sequences sampled from increasingly simplified generative language models, from 4,2,1-layer transformer language models down to language bigrams, revealing a monotonic evolution of the scaling exponents. Our results also include scaling laws obtained from training on random walks on random graphs drawn from Erdős-Renyi and scale-free Barabási-Albert ensembles. Finally, we revisit conventional scaling laws for language modeling, demonstrating that several essential results can be reproduced using 2 layer transformers with context length of 100, provide a critical analysis of various fits used in prior literature, demonstrate an alternative method for obtaining compute optimal curves as compared with current practice in published literature, and provide preliminary evidence that maximal update parameterization may be more parameter efficient than standard parameterization.



1 Introduction

One of the most important lessons in modern deep learning is the steady improvement in model capabilities as additional compute resources and data are effectively leveraged (Sutton, 2019). This was partially quantified through the characterization of neural scaling laws (Cortes et al., 1993; Hestness et al., 2017; Kaplan et al., 2020; Henighan et al., 2020; Hoffmann et al., 2022), which demonstrate that across many vision and natural language tasks, the test loss decreases predictably as a simple power law over many orders of magnitude in number of model parameters N , dataset size D , and amount of compute C . The discovery of neural scaling laws has had significant impact in practice for language model pretraining. It allows practitioners to determine how to optimally scale the model size and dataset size with compute (Kaplan et al., 2020; Hoffmann et al., 2022; Chowdhery et al., 2022; Grattafiori and et al., 2024; Yang and et al., 2024, 2025; Liu and et al., 2024; Jiang and et al., 2024; Tian et al., 2025). It also provides a way to benchmark algorithmic breakthroughs in architectures, optimization, and data.

These empirical results have led to significant theoretical work in trying to understand the origin of neural scaling laws. Specifically, why is there a power law decrease in the test loss over many orders of magnitude in N , D , and C , and what sets the exponents of the power laws? A clear answer to this question may be of significant practical value, since if we understand what sets the exponents, we might understand the extent to which they can be increased, thus increasing the asymptotic efficiency of deep learning methods.

A popular suggestion has been that the power law scaling in the test loss originates from power laws that are already present in the dataset itself. For example, it is well-known that the frequency of words in a corpus

of text follows Zipf’s law, with many other power laws having also been characterized in natural language corpora (Piantadosi, 2014; Altmann and Gerlach, 2016). Natural images also exhibit power laws in their spectra (Ruderman, 1994; Maloney et al., 2022). Many theoretical works have shown that in linear or kernel regression, power laws in the test loss do in fact originate from power laws in the data (or in features defined in terms of the data) (Bordelon et al., 2020; Bahri et al., 2021; Spigler et al., 2020; Maloney et al., 2022; Lin et al., 2024; Paquette et al., 2024; Bordelon et al., 2024). More generally, if we assume that models need to learn a discrete set of tasks to achieve a particular value of test loss, and if these tasks are distributed with power law weighting, then a power law in the test loss follows (Michaud et al., 2024; Ren et al., 2025).

The above theories based on linear models with mean square error (MSE) loss are rather far from the setting of auto-regressive sequence modeling with cross-entropy loss. Consequently it is not clear to what extent they are representative of the neural scaling laws seen in natural language modeling. A potentially fruitful approach would be to study sequence modeling with datasets of *tunable complexity*, where one can systematically dial down from a realistic limit to a highly simplified limit, and track the change in the neural scaling law behavior. An additional benefit of datasets with tunable complexity is that they could potentially allow more appropriate comparisons of models across different scales: a proper comparison of a small model to a large model should also appropriately increase the complexity of the dataset. Complexity of the dataset in turn is not measured simply in terms of size of the dataset, but also in terms of the degree of correlations, and hierarchical, compositional structure (Cagnetta et al., 2024).

To this end, we propose to study sequence modeling of random walks on graphs. Graphs and their generalizations – hypergraphs and hierarchical graphical structures – can capture a large portion of many kinds of data of interest, including many features of language, games, and formal mathematics. In particular, walks on graphs can correspond to generating from n -gram models (Sec. 3), providing a simplified model of language. On the other hand, at a more abstract level, walks on graphs can be used to model stepwise inference and chain of thought reasoning (Khona et al., 2024; Besta et al., 2024).

1.1 Our contributions

Our main contributions are as follows.

- We demonstrate that transformers trained to perform next-token prediction on random walks from random graphs, such as Erdős-Renyi and Barabási-Albert graphs, exhibit neural scaling laws. In particular, we empirically demonstrate the first example of scaling laws even when the input data has no power law structures at all (Fig. 1).
- We systematically reduce the complexity of the language setting by training on progressively simpler generative models of language, measuring the neural scaling laws at each level of complexity (Fig. 2).
- We critically revisit the original neural scaling law results for LLMs and (i) argue that the best fits are one-dimensional fits of the form shown in Eq. 2, in contrast to certain two-dimensional parametric fits that are common in the literature, and (ii) demonstrate a simple neural network regression method to obtain compute optimal scaling laws, which is different from methods presented in the literature to date, and which gives higher accuracy for fitting loss curves (Figs. 10,17,18).
- We demonstrate that the scaling laws for language found in prior work can be accounted for entirely within a 2-layer transformer with a context length of 100. We show in our experiments that the important discrepancy between the Kaplan and Chinchilla scaling laws can be recovered in terms of whether embedding parameters are included (Porian et al., 2024; Pearce and Song, 2024). We also show preliminary results that maximal update parameterization (Yang and Hu, 2021) might be more parameter-efficient than standard parameterization (Figs. 13,14), which would imply that compute-optimal scaling with μP is not at constant number of tokens per parameter.

2 Neural scaling laws

The most well-known and well-characterized neural scaling laws concern the test loss $L(N, D)$, where N and D denote the number of model parameters and the dataset size, respectively. In the context of LLMs, D

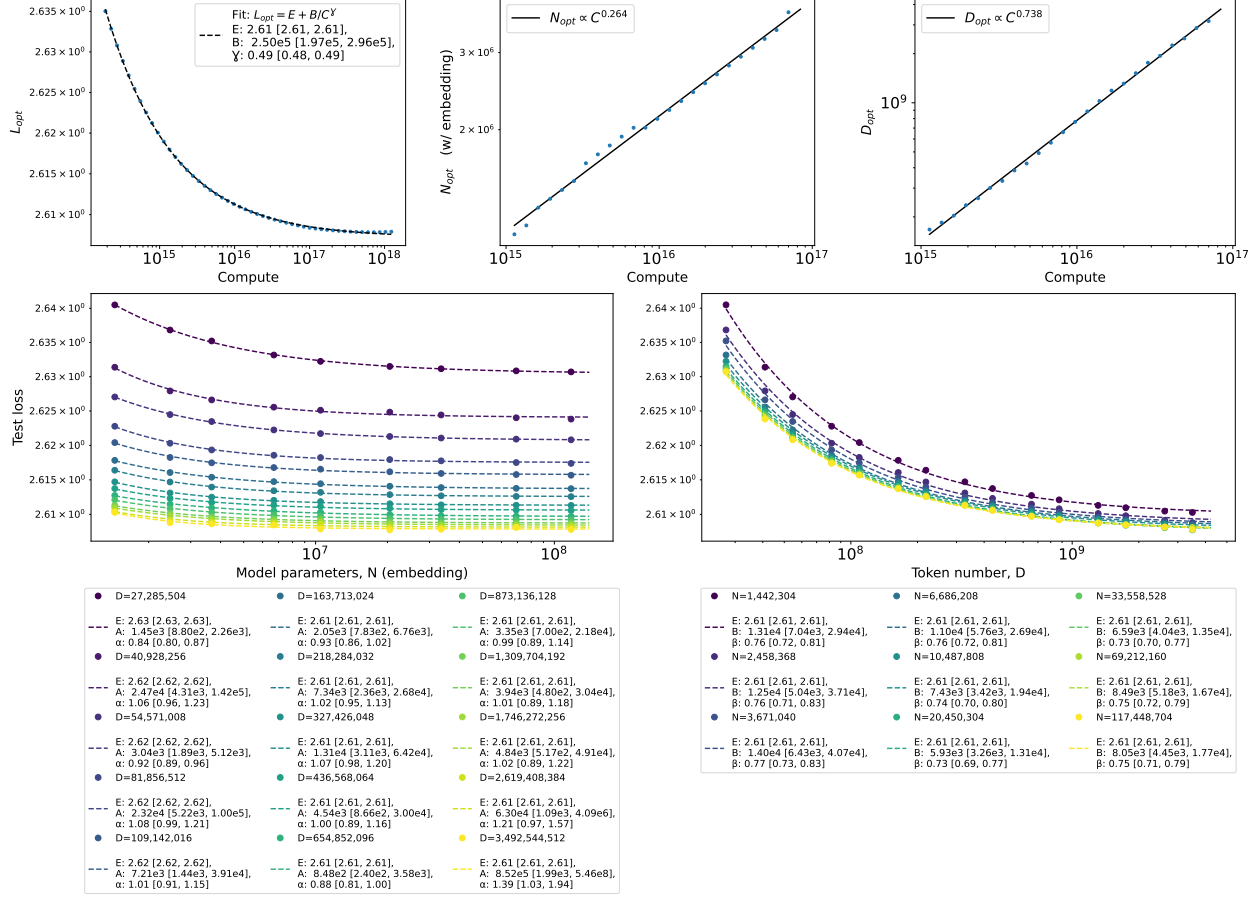


Figure 1 Scaling laws for 2-layer transformers trained on next token prediction on unbiased random walks on an Erdős-Renyi graph, with 8K nodes and 50K edges. Neither the random walks nor the graph exhibits any power laws. Data in bottom two plots are fit to Eq. 2. Mean $\overline{\alpha_D} = 1.028$ with standard deviation 0.129. Mean $\overline{\beta_N} = 0.749$ with standard deviation 0.014. Average MSE for $L(N)_D$ 1d power law fits is 1.07×10^{-8} , compared to 7.03×10^{-8} for best exponential fit. Average MSE for $L(D)_N$ 1d power law fits is 8.86×10^{-8} , compared to 2.13×10^{-6} for best exponential fit. Brackets indicate 95% confidence intervals obtained from bias-corrected and accelerated bootstrap method (see Appendix B for details).

denotes the number of tokens, and N sometimes excludes the embedding parameters. $L(N, D)$ is taken to be the optimal loss over a hyperparameter sweep:

$$L(N, D) = \min_{\{\xi\}} L(N, D; \{\xi\}), \quad (1)$$

where $\{\xi\}$ denote optimization hyperparameters such as learning rate, batch size, weight decay, etc. In practice, one minimizes over a finite grid of hyperparameters. Furthermore, various architectural details, such as aspect ratio, number of attention heads, and so on, are sometimes ignored or held fixed, depending on the study. We denote $L(N)_D$ to be the test loss as a function of N with D held fixed and analogously for $L(D)_N$. Empirically, the test loss is well fit over several orders of magnitude by the equations

$$L(N)_D = E_D + A_D N^{-\alpha_D}, \quad L(D)_N = E_N + B_N D^{-\beta_N} \quad (2)$$

for sufficiently large N or D , respectively. Note that all parameters in this fit depend on the variable that is held fixed. In some cases in the literature, the offsets E_D and E_N are not included, which leads to significant underestimation of the exponents α_D and β_N (see Fig. 9).

It is common to consider two-dimensional parametric fits of the form (Hoffmann et al., 2022; Bhagia et al.,

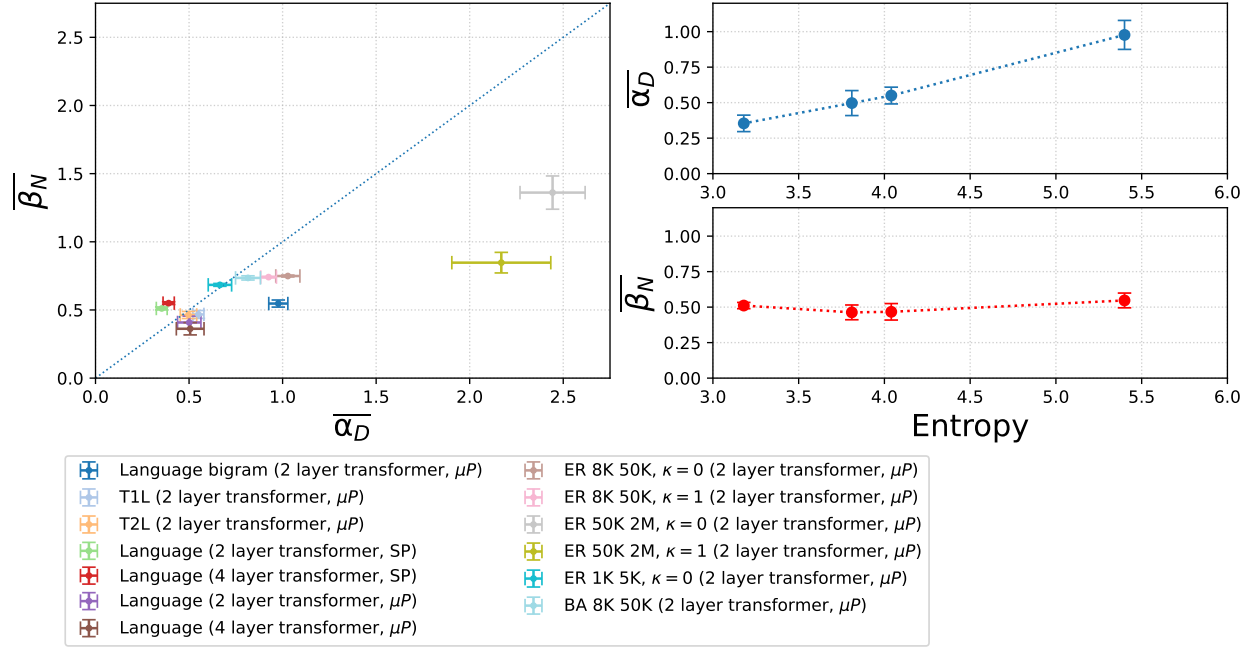


Figure 2 **Left:** Mean exponents $\overline{\alpha_D}$ and $\overline{\beta_N}$ for all experiments reported in this paper. Legend is in the format <dataset> (model). Language refers to Fineweb-edu. $\overline{\alpha_D}$ and $\overline{\beta_N}$ are averages of the best fit exponents α_D and β_N over D and N . Error bars indicate standard deviation of the best fits α_D , β_N across different N and D respectively. **Right:** $\overline{\alpha_D}$ and $\overline{\beta_N}$ for 2-layer transformer experiments on language, T1L, T2L, and language bigrams, demonstrating monotonic evolution of $\overline{\alpha_D}$ with approximate entropy of the dataset, along with relative stability of $\overline{\beta_N} \approx 0.5$.

2025; Muennighoff et al., 2023; Gadre et al., 2024; Zhang et al., 2024; Kang et al., 2025)

$$L(N, D) = E + \frac{A}{N^\alpha} + \frac{B}{D^\beta}, \quad (3)$$

which we refer to as the 2d Chinchilla formula. As we will see, while Eq. 3 is useful for recovering compute optimal scaling curves and has the advantage of being interpretable, it often yields significantly worse fits than other methods, lacks theoretical support and – in some cases – is at odds with theoretical results in simple models (Paquette et al., 2024). (Kaplan et al., 2020) considered a two-dimensional fit of the form

$$L(N, D) = \left[\left(\frac{N_c}{N} \right)^{\alpha/\beta} + \frac{D_c}{D} \right]^\beta \quad (4)$$

for the case of early stopping, although this formula has not been adopted in the literature. The motivation for this formula was to have an analytic expansion in $1/D$ in the large D limit, although there are situations (Hestness et al., 2017; Hutter, 2021) where one expects fractional powers of D in the large D limit. A large variety of other low-dimensional parametric formulas have been considered; see Table 2 of (Li et al., 2024) for a catalog.

The compute in FLOPs (floating point operations) can be expressed exactly in terms of N , D , and number of training steps (Kaplan et al., 2020). It approximately follows the formula $C(N, D) \approx 6NBS$, where S is the number of steps and B is the batch size. For the standard case of 1 epoch training, which we consider hereafter, $D = BS$ and $C(N, D) \approx 6ND$. The compute optimal loss is given by minimizing the loss over N and D subject to a fixed compute:

$$L_{\text{opt}}(C) = \min_{N, D \mid \text{fixed } C} L(N, D). \quad (5)$$

The optimal N and D for a fixed compute are then given by

$$N_{\text{opt}} = \text{argmin}_N L(N, D(C, N)), \quad D_{\text{opt}} = \text{argmin}_D L(N(D, C), N), \quad (6)$$

where in the equation above $N(D, C) \approx C/6D$ refers to N as viewed as a function of D and C , and similarly for $D(N, C) \approx C/6N$. L_{opt} , N_{opt} , and D_{opt} are empirically fit well to

$$L_{\text{opt}} = E_C + KC^{-\gamma}, \quad N_{\text{opt}} = N_0 C^a, \quad D_{\text{opt}} = D_0 C^b, \quad (7)$$

with $a + b \approx 1$.

2.1 Methodology

To extract the scaling laws, we first fit our results for the loss to the 1d parametric fits, Eq. 2. For details regarding the fitting procedure, see Appendix B. We note that fitting a power law does not in general correspond to fitting the loss to a line on a log-log plot. It is crucial to include the irreducible loss, without which one can easily underestimate scaling exponents by over $2\times$ in practice (see Fig. 9).

An important discussion is to what extent the power law fits are accurate (Clauset et al., 2009), especially for their stated purpose of extrapolating predictions for the test loss out to several orders of magnitude in N , D , or C beyond which there is data for $L(N, D)$.¹ In this paper, to validate the power law fit, we compare it to an exponential fit of the form $f(x) = a + be^{-cx}$. The ratio between the mean squared error (MSE) of the power law and exponential fits are depicted in Fig. 15. In all cases studied in this paper, the best power law fits for $L(D)_N$ have factors of 50-100x better MSEs than the best exponential fits; for $L(N)_D$, with one exception the power law fits have factors of 5-100x better MSEs than the exponential fits. An important message of our paper is that next-token prediction on various types of random walks gives power law fits to the loss that are nearly as good from the perspective of MSE – and in some cases better – than those for natural language.

To obtain compute optimal fits requires more analysis, because in practice we have not sampled enough values of N , D . In the next step, we obtain a prediction $\hat{L}(N, D)$ for values of N, D that are not in the raw dataset. To obtain this prediction, instead of using the 2d fits of Eq. 3, 4 as is common in the literature, we use an alternative technique – regression with a 3-layer fully connected neural network (for details see Appendix B). We demonstrate that this method (along with a kernel regression method) gives significantly better train/validation errors than the 2d Chinchilla fit that is widely used in the literature (see Figs. 10, 17, 18). Since the 2d Chinchilla fit does not have a strong theoretical basis, we suggest eschewing it in favor of more standard ML regression techniques. Given $\hat{L}(N, D)$, we can then use a sufficiently fine grid for N, D to extract compute optimal scaling laws following Eqs. 5, 6, 7.

In all of our figure captions we report the mean exponents $\overline{\alpha_D}$ and $\overline{\beta_N}$, which are the average of the best-fit exponents α_D and β_N across different values of D and N . We also report the standard deviation for the best fit α_D and β_N across different values of D and N , which are the error bars in Fig. 2. Note that these standard deviations do not take into account the confidence intervals for each fit, which are shown in brackets in the figure legends.

Details of our experiments are presented in Appendix A. We use a decoder-only GPT-style transformer to perform next-token prediction. We use settings characteristic of standard language pretraining (Brown et al., 2020; Hoffmann et al., 2022), including 1 epoch training with a learning rate schedule consisting of linear warmup and cosine decay. In all of our figures, “Compute” refers to the number of FLOPs (floating point operations), “ N (embedding)” refers to the total number of parameters including embedding parameters, while “ N (non-embedding)” excludes the embedding parameter count.

3 Random walks, n -grams, and random graphs

The simplest non-trivial generative model of sequences is a Markov random walk on a graph. Consider a directed, weighted graph on N nodes with weight matrix W_{uv} . We can sample a random walk by randomly starting at a node with some initial distribution and then iteratively sampling from the probability distribution $p(u|v) := W_{uv} / \sum_u W_{uv}$.

¹Note that the number of orders of magnitude covered by N can change significantly depending on whether N includes embedding parameters. Compare for example Fig. 11 with 12.

Observe that the above is equivalent to generating from a bigram model. Recall that an n -gram language model approximates the conditional joint distribution of text in terms of the $n - 1$ most recent tokens: $p(x_t|x_{t-1}, \dots, x_0) = p_n(x_t|x_{t-1}, \dots, x_{t-n+1})$. In the case of a bigram model ($n = 2$), this defines a directed, weighted graph, which we refer to as the bigram graph. For a vocabulary of size V , the bigram graph has V nodes, and each directed edge uv is associated with a weight $p_2(u, v)$. Sampling from a bigram model corresponds to sampling a random walk on the bigram graph, with transition probabilities $p(u|v) = p_2(u, v)/p_1(v)$, where $p_1(v) = \sum_u p_2(u, v)$ is the stationary distribution on nodes, and equivalently the unigram distribution of the sequence.

This picture can be readily generalized to $n > 2$. In that case, the n -gram model defines a directed, weighted hypergraph with V nodes. Directed n -hyperedges, which consist of ordered n -tuples (x_1, \dots, x_n) , are associated with a weight $p_n(x_n, \dots, x_1)$. Sampling from the n -gram model then consists of sampling a random walk on the hypergraph: given $n - 1$ nodes $x_{t-1}, \dots, x_{t-n+1}$, a hyperedge is chosen at random, giving the next node x_t in the sequence. The initial $n - 1$ nodes can be chosen from the stationary joint distribution on $n - 1$ nodes.

Next-token prediction on a random walk on an ordinary graph ($n = 2$) is essentially a problem of learning a probability table. Given training sequences $\{x_1^{(i)}, \dots, x_T^{(i)}\}$, for $i = 1, \dots, N_{\text{seq}}$, the task requires the model to learn that they are controlled by bigram transition probabilities $p(u|v)$ and then to learn the probabilities themselves. The obvious algorithm to learn this is to form a prediction \hat{p} by counting co-occurrences in the training set, which is exactly how bigram models are learned (Jurafsky and Martin, 2009). If we consider a cross-entropy or MSE loss function L comparing the prediction \hat{p} to the ground truth p , then in expectation over a sample of size D tokens,

$$\mathbb{E}[L] = E + B/D + O(1/D^2), \quad (8)$$

as shown in Appendix C. For cross-entropy loss, E is the entropy of the distribution p , while for MSE loss $E = 0$. B is a constant depending on $|V|$. This provides a baseline against which we can compare our empirical results. Note that this can be thought of as the "variance-limited" regime for power law scaling of data in the language of (Bahri et al., 2021).

An unbiased random walk on an undirected graph has the transition probability $p(u|v) = \frac{A_{uv}}{\deg(v)}$, where A is the adjacency matrix and $\deg(v) = \sum_u A_{uv}$ is the degree of v . The stationary distribution is $p(u) = \frac{\deg(u)}{2E}$, where E is the number of edges in the graph. Recall that random walks have an exponentially decaying auto-correlation, with the time-scale for the exponential decay set by the spectral gap of the transition matrix.

3.1 Random graphs: Erdős-Renyi and Barabási-Albert ensembles

In order to understand better the scaling laws of language models, it is interesting to compare their performance to a simple baseline of learning random walks on random graphs.

3.1.1 Erdős-Renyi graphs

The simplest class of random graphs are Erdős-Renyi graphs. The number of nodes is denoted N . The adjacency matrix of the graph is chosen randomly such that $A_{ij} = 1$ with probability p and 0 with probability $1 - p$. The degree distribution of the nodes is tightly concentrated around the expected degree, $\langle k \rangle = p(N - 1)$, and the expected number of edges is $\langle E \rangle = \langle k \rangle N/2 = pN(N - 1)/2$. The spectrum of the adjacency matrix obeys a semicircle law, which is typical of random symmetric matrices. Neither the degree distribution nor the spectrum of the graph has any power laws. In Fig. 3 we present the degree distribution (equivalent to the unigram distribution for unbiased walks) and the bigram distribution ($p(u|v)$) for an unbiased random walk on an ER graph with $N = 8,192$ and $E = 53,292$ that we use in our experiments, demonstrating the absence of any power law structure in the input data correlations.

Our first main result is presented in Fig. 1, demonstrating the existence of neural scaling law behavior. This result demonstrates that neural scaling laws are a generic feature of learning sequence models with cross-entropy loss, *independent of whether the data itself has any power law structure*. These models were trained with maximal update parameterization (μP) with context length of 50; additional experimental details are presented in Appendix A.

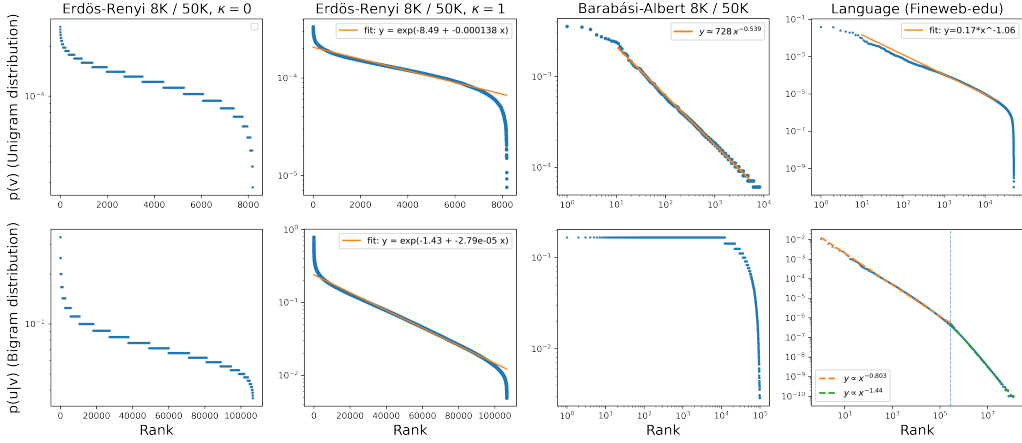


Figure 3 Stationary distribution on nodes $p(v)$ (unigram distribution) and transition probability distributions $p(u|v)$ (bigram distribution) plotted against the rank for various representative cases studied in this paper. Note that $p(v)$ is equal (up to an overall constant) to the degree distribution of the graph when $\kappa = 0$. Left two columns are plotted on log-linear scale, and the right two columns are on log-log scale. ER ($\kappa = 0$) case is tightly concentrated around its mean probability, as indicated by roughly constant size plateaus. BA ($\kappa = 0$) has power laws in both unigram and bigram distributions; the unigram exponent is approximately equal to the theoretical expectation $1/(\gamma - 1) = 0.5$. The power law in the bigram is more clear if plotted in reverse rank order (not shown), but can be observed from the decreasing width of the plateaus. Language results are from Fineweb-edu using GPT-2 tokenizer; unigram distribution is a standard Zipf plot, while bigram distribution shows broken power law.

We have studied unbiased random walks on ER graphs of varying sizes. Fig. 22 demonstrates results from an ER graph with $N = 50,000$ and $E = 2M$ edges. We also present results for ER graphs with 1K nodes and 5K edges in Fig 5; this in particular demonstrates that scaling laws in these settings can already be observed at relatively small scales, which should be accessible at relatively low compute levels ($10^{13} - 10^{16}$ FLOPs in our experiments).

3.1.2 Biased random walks: dialing into power laws

We can controllably tune the stationary distribution (equivalently, unigram distribution) $p(v)$ and the transition probabilities $p(u|v)$ (equivalently, bigram distribution) by considering biased random walks. We consider sampling a weight matrix W_{uv} from a power-law distribution $\Pr(W_{uv} = k) \propto k^{-\kappa}$, for $k \in [k_{\min}, k_{\max}]$ and 0 otherwise (when the edge uv is present in the graph). For $\kappa > 1$, the transition probabilities follow a power law distribution, $P(u|v) \propto (1/r_{(u|v)})^{\frac{1}{\kappa-1}}$, where $r_{(u|v)}$ is the rank of the bigram $(u|v)$, sorted from highest to lowest in probability. $\kappa = 1$ is the marginal case, where the probabilities and their ranks follow an exponential (log-linear) relationship: $P(u|v) = P_0 e^{-s r_{(u|v)}}$, for constants s, P_0 .

We present results for the marginal case $\kappa = 1$. The unigram and bigram distributions for the ER graph with 8K nodes and 50K edges are shown in Fig 3, which shows that $\kappa = 1$ smooths the unigram and bigram distributions compared to the case $\kappa = 0$. This is an interesting intermediate case: on the one hand the data correlations still lack power laws, on the other hand they sit in between the $\kappa = 0$ case and the case where the unigram and bigram distributions do have power laws.

The scaling law results for the marginal case $\kappa = 1$ are shown in Fig. 4 for the 8K / 50K graph and in Fig. 23 for the 50K / 2M graph. The primary observation is that the quality of the power law fits are improved (see, e.g. Fig. 15), suggesting that the structure of the data correlations can help crystallize the power law scaling in the loss. It would be interesting to continuously tune the exponent κ and see the evolution in the scaling exponents and the quality of the fit, which we leave for future work.

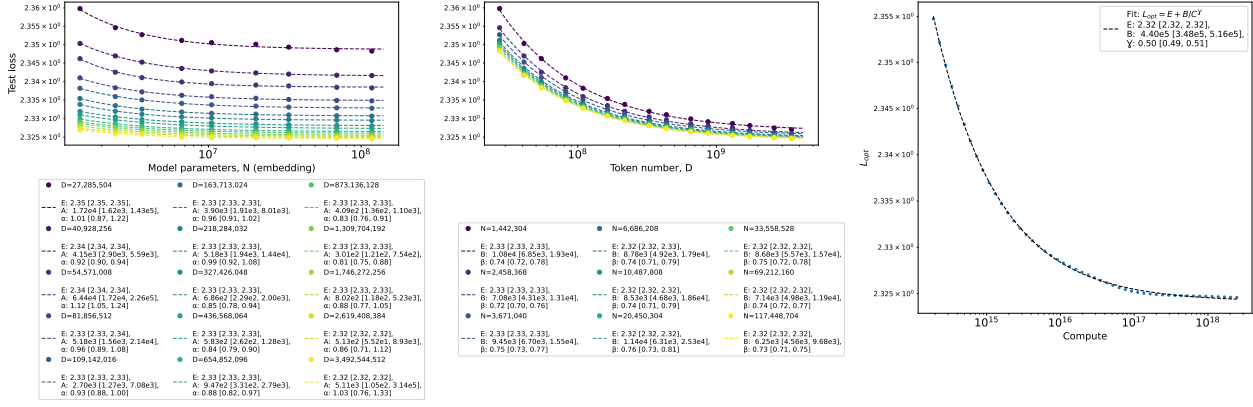


Figure 4 Scaling laws for Erdos-Renyi graph with 8K nodes and 50K edges, with power-law transition probabilities set by $\kappa = 1$. Mean exponent $\overline{\alpha_D} = 0.925$ with standard deviation 0.084. Mean exponent $\overline{\beta_D} = 0.741$, with standard deviation 0.010. Average MSE for $L(N)_D$ 1d power law fits is 1.76×10^{-8} , compared to 1.03×10^{-7} for best exponential fit. Average MSE for $L(D)_N$ 1d power law fits: 5.15×10^{-8} , compared to 2.12×10^{-6} for best exponential fit.

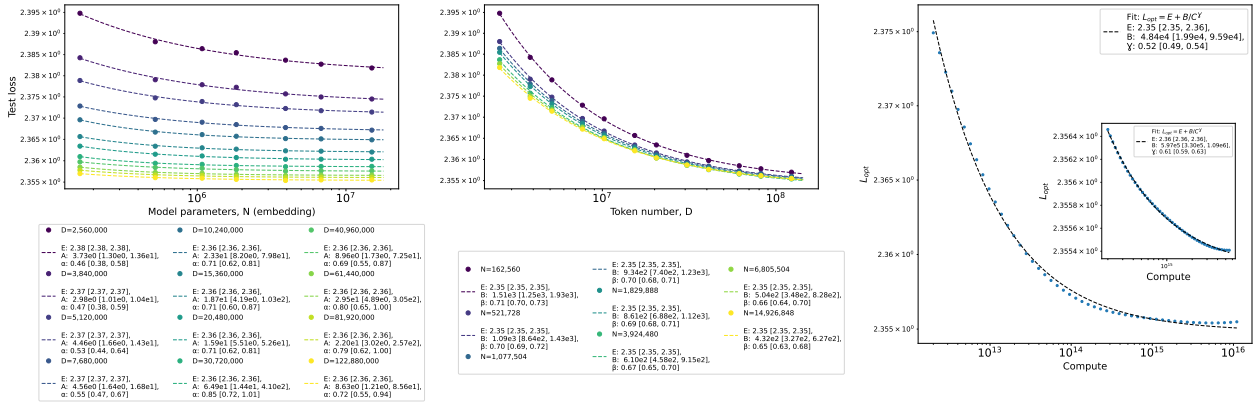


Figure 5 Scaling laws for unbiased ($\kappa = 0$) random walk on Erdos-Renyi graph with 1K nodes and 5K edges. Mean exponent $\overline{\alpha_D} = 0.665$ with standard deviation 0.125. Mean exponent $\overline{\beta_D} = 0.684$, with standard deviation 0.021. Average MSE for $L(N)_D$ 1d power law fits is 2.41×10^{-8} , compared to 1.96×10^{-7} for best exponential fit. Average MSE for $L(D)_N$ 1d power law fits: 3.37×10^{-8} , compared to 1.97×10^{-6} for best exponential fit.

3.1.3 Scale-free graphs: Barabási-Albert ensemble

Another way to introduce power law structures in the data is to introduce it in the connectivity structure of the graph itself. A scale-free graph (Barabási and Albert, 1999) is defined such that a randomly chosen node has degree k with probability $\propto k^{-\gamma}$ for large k , with $\gamma > 1$. Typical examples of approximately scale-free graphs include the world wide web inward-directed edges, protein-protein interactomes, and the in-degree of citation networks for academic papers. Co-occurrence matrices from natural language corpora in particular have been shown to determine a scale-free, small-world graph (Cancho and Solé, 2001). One way to construct a scale-free graph is via the Barabási-Albert preferential attachment model (Barabási and Albert, 1999), which gives $\gamma = 3$. We use this model to construct a scale-free graph with 8,192 nodes and 49,131 edges. We display the power-law unigram and bigram distributions for the unbiased ($\kappa = 0$) walk in Fig. 3. The resulting scaling laws for learning unbiased random walks on this graph are presented in Fig. 21. Qualitatively the results are similar to the ER graphs without power law structures, and in fact the power law fit is somewhat worse for $L(N)_D$ (Fig. 15).

4 Dialing up complexity: from random graphs to natural language

It is of great interest to understand the origin of the neural scaling laws and to what extent the scaling exponents can be altered by the architecture, data and learning algorithms. One way forward is to develop methods to define and tune the complexity of the dataset and to study how the scaling exponents vary. At the high level of complexity are real-world datasets, like natural language, math, and coding datasets. At the low end of complexity are bigram models, which are equivalent to Markov random walks on graphs. In this paper we consider a monotonic dialing up of the complexity of language models. At the lowest level of complexity we start with a bigram language model. At an intermediate level of complexity, we consider a synthetic dataset generated from sampling the outputs of an n -layer transformer trained on FineWeb-edu (Penedo et al., 2024). For a sufficiently large transformer, given the stunning success of transformer-based large language models, these sequences should approximate natural language quite closely. For small transformers they presumably provide a synthetic dataset of intermediate complexity. In this paper we study the case $n = 1, 2, 4$, and refer to these datasets as Transformer-generated n -layer (TnL) datasets.

One can imagine other generative models that also interpolate complexity from bigram models to natural language: n -gram models for $n > 2$ and hierarchical graphical models of natural language. We leave the study of scaling laws for these cases to future work.

As a rough measure of the complexity, we use the entropy of the joint distribution of the sequences in the dataset. We think of this as a rough measure of complexity because a low complexity dataset has low signal in predicting x_t from x_{t-1}, x_{t-2}, \dots , giving rise to many likely possibilities and therefore high entropy. On the other hand, a high complexity dataset has high signal in predicting x_t from x_{t-1}, x_{t-2}, \dots , and therefore the entropy should be lowered. Indeed, it is easy to show that for an n -gram language model, the entropy monotonically decreases with n .

While one can define and compute the entropy of an n -gram model, it is not feasible to compute the entropy of the sequences generated by TnL since it would require a number of samples that is exponential in the sequence length. Even worse, the entropy of natural language does not have an intrinsic definition, since there is no true generative model that one can use to define a joint distribution. We can, however, approximate the entropies by recalling that the cross-entropy loss is lower-bounded by the entropy of the reference distribution. Therefore, if we fit power laws $L(N)_D = E_D + A_D/N^{\alpha_D}$, and $L(D)_N = E_N + B_N/D^{\beta_N}$, the entropy of the reference distribution can be approximated as $E = \lim_{N \rightarrow \infty} E_N = \lim_{D \rightarrow \infty} E_D$. As a rough estimate, we take the smallest value of E_N or E_D that appear in our fits and use that as a proxy for the entropy E . This gives $E = 5.40, 4.04, 3.81, 3.18$ for the bigram language model, T1L, T2L, and natural language (Fineweb-edu), respectively, which is consistent with our expectation that these generative models have increasingly higher complexity.

4.1 Scaling laws for learning language bigrams

Here we discuss our results for scaling laws for next-token prediction on sequences generated from a bigram language model. To define our bigram language model, we use the GPT-2 tokenizer (Radford et al., 2019), which has a vocabulary of size 50,257. We train our bigram model on the Fineweb-edu-10B dataset (Penedo et al., 2024). This dataset has approximately 130M unique bigrams. Fig. 3 (bottom right) displays the bigram probabilities $p(u, v)$ vs. their rank, showing a (broken) power-law distribution. As depicted in Fig. 19, a large number of bigrams appear only a handful of times; for our work to be computationally tractable, we remove all bigrams that appear 5 times or fewer, leaving around 33M unique bigrams. Therefore, our truncated bigram model corresponds to a graph with approximately 50K nodes and 33M edges, and with a (broken) power law weight matrix.

The scaling laws for learning using a 2-layer transformer with maximal update parameterization (μP), a context length of 50, and a fixed batch size of 100 sequences are shown in Fig. 6. The exponents α_D lie in the range $0.84 - 1.2$. The mean and standard deviation of the best fit exponents across the different values of D are $\overline{\alpha_D} = 0.977$, $\sigma_{\alpha_D} = 0.102$ respectively. The β_N lie in the range $0.47 - 0.60$, with mean $\overline{\beta_N} = 0.547$ and standard deviation $\sigma_{\beta_N} = 0.052$. While the α_N 's are significantly higher than natural language, the β 's are much closer. Interestingly, this language bigram example shows the clearest power law fits. As depicted in

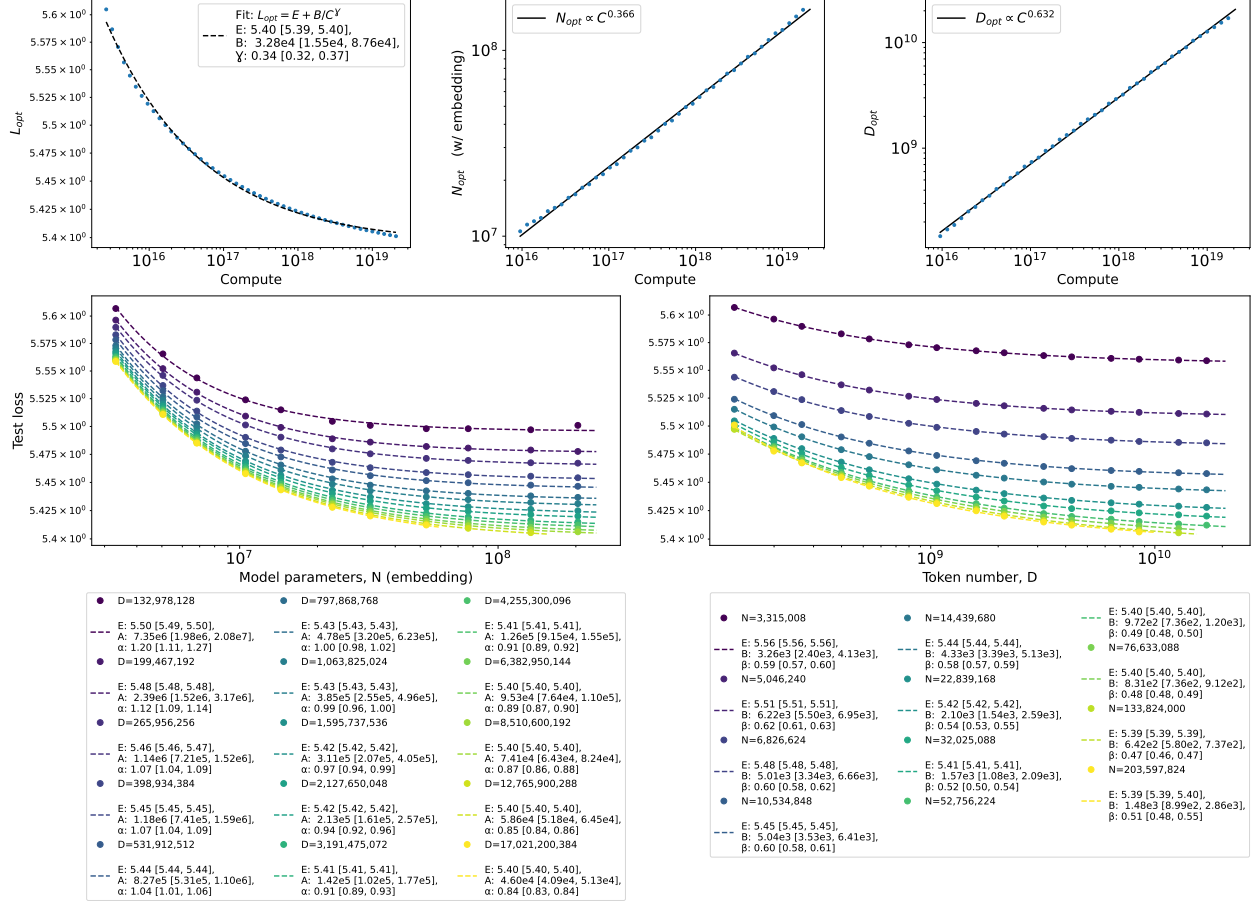


Figure 6 2 layer transformer trained on language bigram with μP . The α_D have a mean of $\overline{\alpha_D} = 0.977$ and a standard deviation of 0.102. The β_N have a mean of $\overline{\beta_N} = 0.547$ and a standard deviation of 0.052. Average MSE for $L(N)_D$ 1d power law fit is 5.22×10^{-7} , as compared to 2.91×10^{-5} for the best exponential fit. Average MSE for $L(D)_N$ 1d power law fits is 1.66×10^{-7} , as compared to 6.51×10^{-5} for the best exponential fit.

Fig. 15, the ratio of the MSE between the best power-law and best exponential fits are 0.0179 and 0.0026, respectively.

The compute optimal curves also demonstrate that learning the bigram model is much more compute efficient than natural language, as the exponent γ is substantially larger, and also more parameter efficient, as a is almost half as large as b .

4.2 Scaling laws for learning TnL-Language

Here we discuss our results for scaling laws for 2-layer transformers learning TnL sequences. These experiments had the same settings as the language bigram experiments: μP parameterization with a context length of 50 and a fixed batch size of 100 sequences. Fig. 7 and 8 show the case with $n = 1$ and 2 respectively.

As summarized in Fig. 2, we found that the mean of exponents $\overline{\alpha_D}$ interpolate between the language bigram and natural language results.

The results for T4L were nearly identical to those for T2L, so we omit them from the presentation. We expect the reason is that a 2-layer transformer may not be able to clearly distinguish between sequences generated from a 2-layer and 4-layer transformer

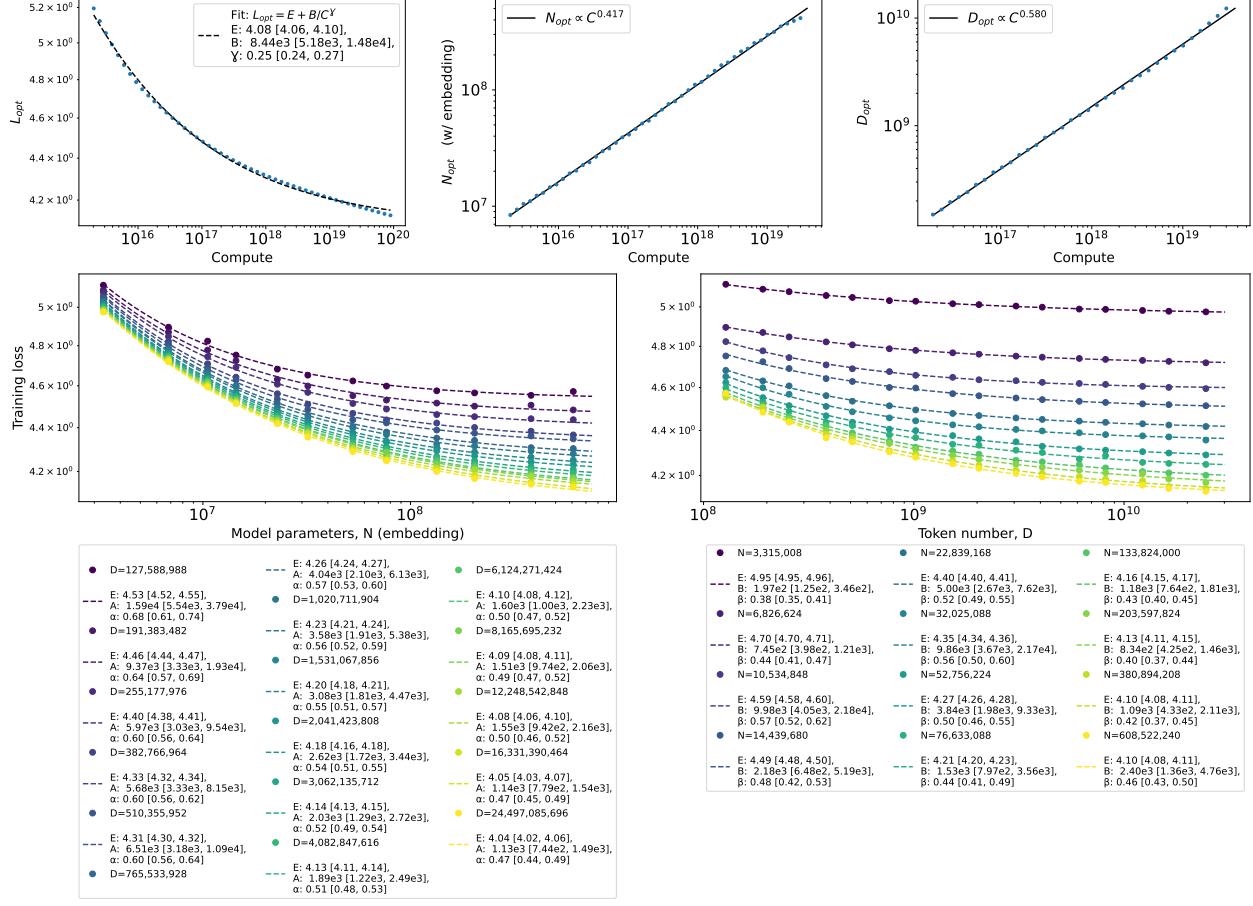


Figure 7 Scaling laws for 2 layer transformers learning T1L. The α_D have a mean of 0.550, with a standard deviation of 0.059. The β_N have a mean of 0.467, with standard deviation 0.058. The average MSE for the $L(N)_D$ 1d power law fits is 6.84×10^{-5} , while the average MSE for the best fit exponential fit is 1.49×10^{-3} . Average MSE for $L(D)_N$ 1d power law fits is 2.13×10^{-5} , compared to 1.27×10^{-3} for the best exponential fit.

5 Revisiting scaling laws for natural language modeling

In this section we present our results on neural scaling laws for LLM pretraining. Scaling laws for natural language modeling have been well-studied in the literature; the primary purpose of our discussion here is twofold. One is to explain our methodology while providing a critical analysis of some widely used methodology in the literature. The other is to demonstrate how the results in the previous sections directly compare to the setting with natural language. Specifically, we present four main points:

1. Dropping the constants E (referred to as the irreducible loss) in the 1d fits, as done in some prior works, leads to dramatic underestimation of the scaling exponents and significantly poorer fits. Consequently, power-law scaling in the loss should not show up as a clean line on a log-log plot, but rather have curvature, as shown in all our results.
2. The two-dimensional Chinchilla formula in general gives poor fits compared to other standard ML methods, in addition to having no theoretical basis. We suggest replacing the 2d Chinchilla formula with neural network regression to fit $L(N, D)$, which is the methodology used in this paper to obtain compute-optimal scaling results.
3. Many prior results in neural scaling laws – including the discrepancy between (Hoffmann et al., 2022) and (Kaplan et al., 2020) – can be largely recovered from training shallow transformers (2 layers) with short context lengths (context length 100); in our experiments, resolving the discrepancy does not

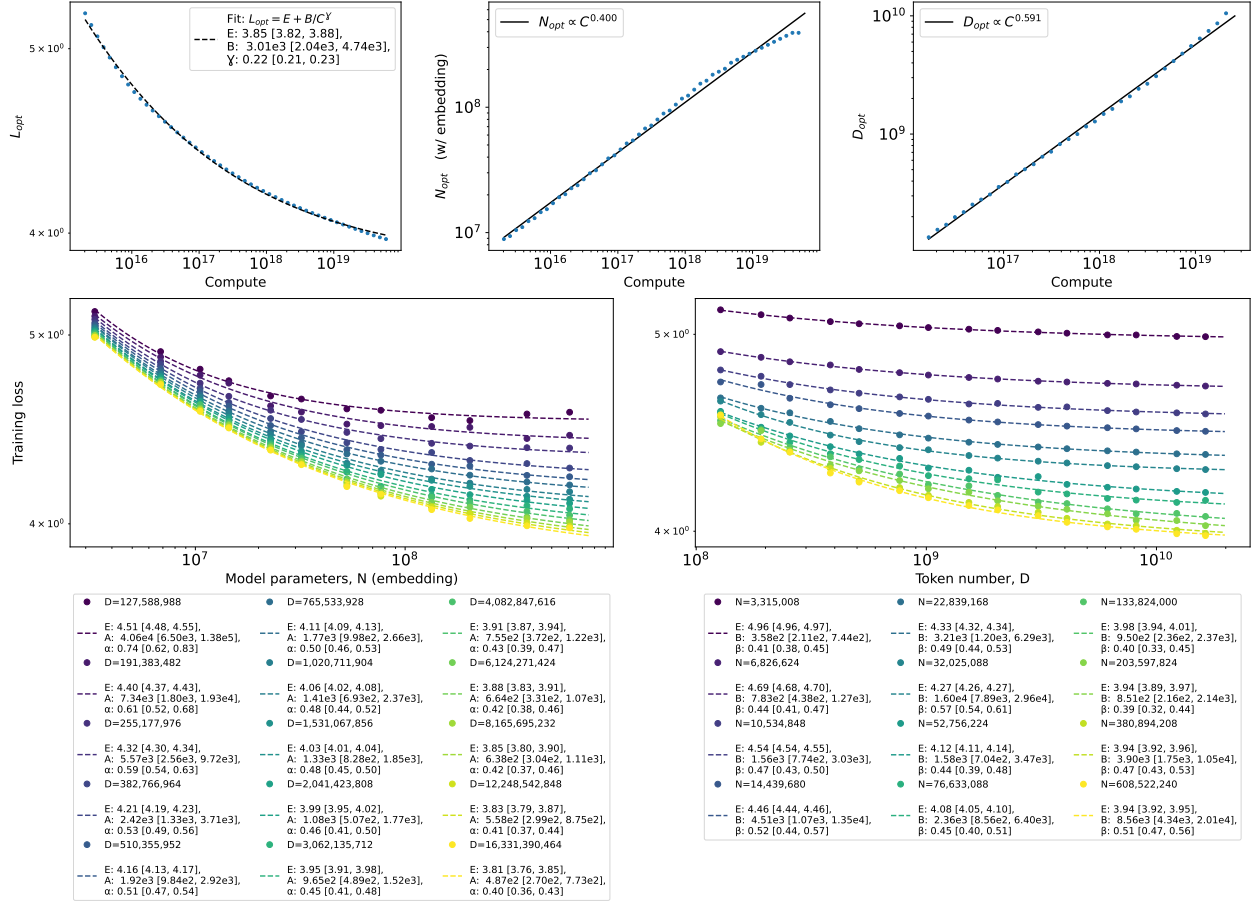


Figure 8 2 layer transformer train on T2L. The mean α_D is 0.497, with standard deviation 0.088. The mean β_N is 0.463 with standard deviation 0.052. The average MSE for $L(N)_D$ 1d power law fits is 1.91×10^{-4} , compared to 2.03×10^{-3} for the best exponential fit. Average MSE for $L(D)_N$ 1d power law fits is 6.22×10^{-5} , compared to 1.52×10^{-3} for the best exponential fits.

require changing the learning rate schedule as discussed in many works.

4. We find preliminary evidence that using maximal update μP parameterization (Yang and Hu, 2021) may be more parameter efficient for compute optimal training.

5.1 Importance of the irreducible loss

To make the first point (1) above, we consider six models in the Pythia sequence of LLMs (Biderman et al., 2023), which were trained on 300B tokens from the Pile dataset. Using the data provided by (Michaud et al., 2024), we consider the 1d fit $L(N)_D$ both with and without the offset E_D . Neglecting the offset E_D as in (Michaud et al., 2024) gives a nearly factor of two difference in the scaling exponent and almost an order of magnitude difference in the mean squared error (MSE) of the fit. We note that an exponent of $\alpha = 0.07$ was presented in (Henighan et al., 2020) (see top left of Fig. 3 in (Henighan et al., 2020)) upon neglecting E_D , and we expect a similar conclusion to hold in that case as well.

An important upshot of this discussion is that while it is common to present power-law scaling as a linear fit to the loss on a log-log plot, more accurately the fit should be curved. One could attempt to fit a line to the reducible loss, $L - E$, however this requires an extremely accurate estimate of E , particularly in the tails of the power law, which is often not available without first finding the best fit for L .

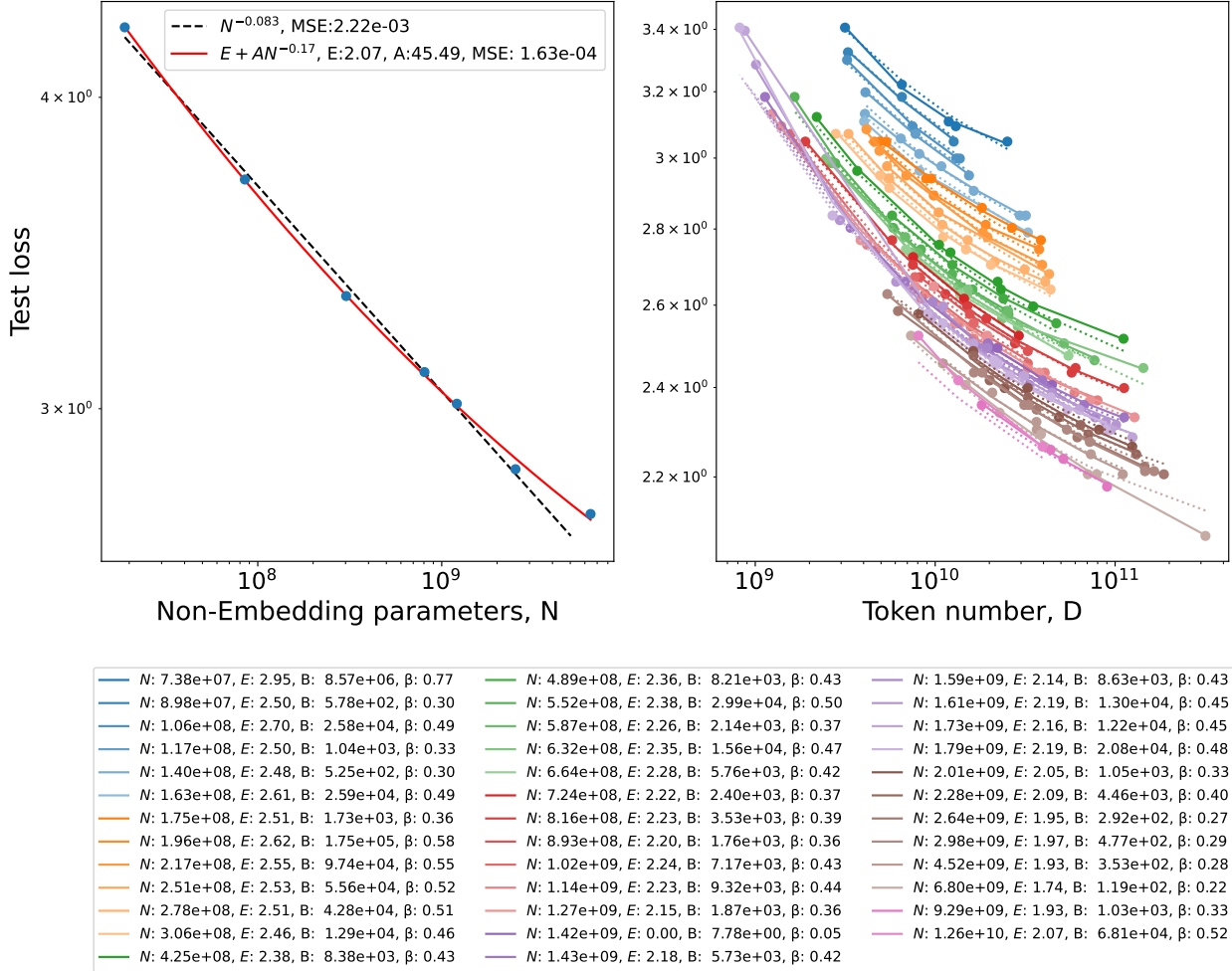


Figure 9 Left: Fits for $L(N)_D$ for the Pythia models. Right: 1d $L(D)_N$ fits for Chinchilla data (solid lines) with parameters shown in the legend, $L(N, D)$ fits to 2d Chinchilla formula (dotted lines). N includes embedding parameters.

5.2 2d Chinchilla fit is relatively poor

Next, to address point (2) above, we revisit the Chinchilla results (Hoffmann et al., 2022). The raw data for $L(N, D)$ reported in (Hoffmann et al., 2022) was extracted and shared in (Besiroglu et al., 2024), which we used for our analysis below. First, we compare three different methods for fitting a two-dimensional function $L(N, D)$, which allows determination of the compute optimal scaling laws: (i) fitting to the 2d Chinchilla formula, Eq. 3, (ii) neural network regression, and (iii) kernel regression. We refer to Appendix B for details regarding the neural network and kernel fits. The raw Chinchilla data contains 245 pairs of (N, D) values. Following (Besiroglu et al., 2024), we throw out the datapoints corresponding to the 5 largest values of $L(N, D)$, which appear to be outliers due to poor optimization.

In all three cases, we perform an 80/20 train/validation split on the data, fit using a Huber loss ($\delta = 10^{-3}$) as in (Hoffmann et al., 2022), and report the MSE test loss averaged over 20 random splits. We note that such classical machine learning methods are not typically reported in the contemporary neural scaling law literature. The train / validation MSEs, averaged over the 20 train / validation splits, are displayed in Fig. 10. We see that the neural network and kernel fits gives an almost 2 \times factor improvement in the average validation MSE. From a model selection perspective, one should use the kernel or neural network fit over the 2d Chinchilla fit.

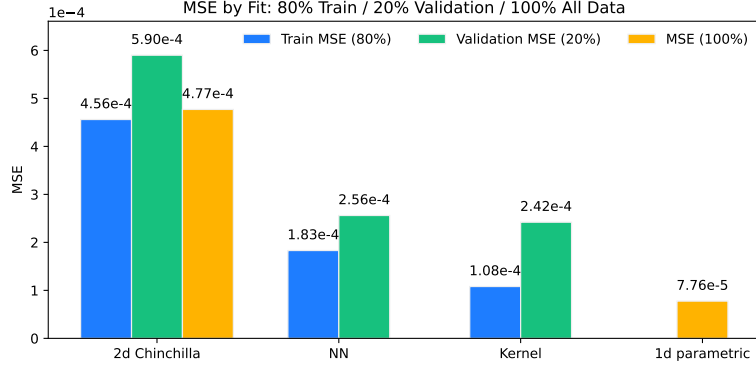


Figure 10 Train and validation MSEs for the 2d Chinchilla fit, neural network regression, kernel regression, and the 1d parametric fit of Eq. 2, for the Chinchilla data (Hoffmann et al., 2022; Besiroglu et al., 2024).

The drawback of the neural network and kernel fits are that they are not interpretable. To also have interpretable conclusions, we consider the one-dimensional fit $L(D)_N$ given in Eq. 2. The result is plotted in Fig. 9 and the MSE is shown in Fig. 10. The 1d equations give a significantly better fit, with a MSE of 7.76×10^{-5} . This is almost an order of magnitude better than the 2d fit, which gives an MSE of 4.77×10^{-4} . This is unsurprising given that there are many more parameters, but also indicates that it is more accurate to consider an exponent β_N varying with N .

The 2d fit yields the parameters $A = 477.82$, $B = 2143.62$, $E = 1.8172$, $\alpha = 0.3473$, $\beta = 0.3672$. The 1d fit, $L(D)_N = E_N + BD^{-\beta_N}$ gives a range of exponents, $\beta_N \sim 0.3 - 0.6$, albeit with some outliers; specifically, mean $\overline{\beta_N} = 0.41$ and standard deviation 0.085 after throwing out the two extreme outliers. While these are consistent with each other, we see β_N does have considerable variation with N . There are not enough datapoints for fixed D to obtain a fit for $L(N)_D$.

One can also use the neural network or kernel fits to extract compute optimal curves, using the methodology described in Sec. 2.1. In Appendix B.4 Fig. 16, we present the results for compute optimal curves computed using the neural network fit to $L(N, D)$. Our method yields the exponents $\gamma = 0.16$, $a = 0.482$, $b = 0.504$. These results are in relatively good agreement with the 2d Chinchilla fit ($\gamma = \frac{\alpha\beta}{\alpha+\beta} = 0.178$, $a = \frac{\beta}{\alpha+\beta} = 0.513$, $b = \frac{\alpha}{\alpha+\beta} = 0.487$).

5.3 Recovering basic scaling law results with 2 layer transformers and short context lengths

Here we discuss the findings summarized in point (3) at the beginning of this section. We train a 2 layer transformer with context length 100, using a fixed batch size of 512 sequences, with standard parameterization. We use embedding dimensions $n_{\text{embd}} = 64, 128, 256, 512, 1024, 2048$. The number of attention heads is $\max(4, n_{\text{embd}}/64)$.

The 1d fits for $L(N)_D$ and $L(D)_N$, where N either includes embedding parameters or not, are shown in Figs. 11, 12. The α_D are in the range $\alpha_D \sim 0.29 - 0.46$, with a mean of $\overline{\alpha_D} = 0.354$, which is close to the result for α from the 2d Chinchilla fit. The β_N are in the range $0.48 - 0.55$, with a mean $\overline{\beta_N} = 0.511$. These are slightly higher, but within the same range, than the results in the preceding section where we refit the Chinchilla data.

The 2D Chinchilla fit yields the parameters $A \approx 507$, $B = 20094$, $E = 2.802$, $\alpha = 0.365$, $\beta = 0.503$. The exponents α, β are close to the means $\overline{\alpha_D}, \overline{\beta_N}$ obtained from the 1d fits. These imply the compute optimal exponents $L_{\text{opt}} \sim C^\gamma$ with $\gamma = \frac{\alpha\beta}{\alpha+\beta} = 0.212$. In Fig. 11, we present the compute optimal scaling curves obtained using the neural network fit (including embedding parameters), which is within 20% of the prediction from the 2d Chinchilla formula.

Figs. 11, 12 also depict the scaling exponents for the optimal parameter and data size as a function of compute, $N_{\text{opt}} \sim C^a$, $D_{\text{opt}} \sim C^b$, for both the case where embedding parameters are and are not included. From the fits, we see that when embedding parameters are included, we have $a/b \approx 0.94$, which is close to the famous Chinchilla result that $a/b \approx 1$. When embedding parameters are not included, we have $(a, b) = (0.742, 0.386)$,

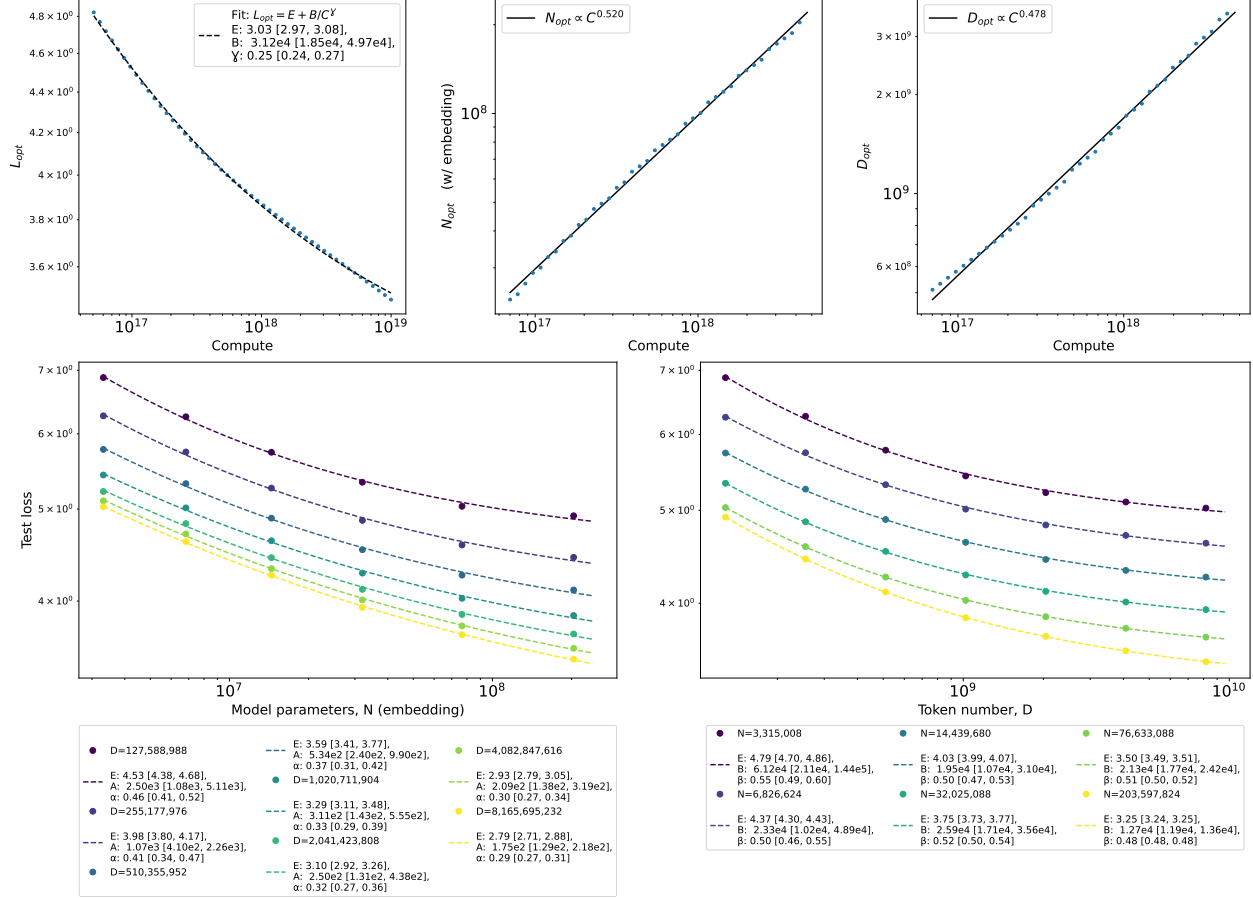


Figure 11 2 layer transformer trained on language with *SP*, where N includes the embedding parameters. Mean exponent $\bar{\alpha}_D = 0.354$ with standard deviation 0.058. Mean exponent $\beta_N = 0.511$ with standard deviation 0.022. Average MSE for $L(N)_D$ 1d power law fits is 5.41×10^{-4} . Average MSE for $L(N)_D$ 1d exp fits: 6.09×10^{-3} . Average MSE for $L(D)_N$ 1d power law fits: 1.88×10^{-4} . Average MSE for $L(D)_N$ 1d exponential fits: 1.00×10^{-2} .

which is close to the OpenAI result of $(0.73, 0.27)$ (Kaplan et al., 2020). Our result is in line with observations in (Porian et al., 2024; Pearce and Song, 2024), that a major part of the discrepancy between the Chinchilla and OpenAI scaling laws is whether embedding parameters are included. These prior works also identified learning rate schedules and other factors in contributing to the discrepancy; in light of our results, these might be more relevant for deeper models.

5.4 Scaling laws with μP : improved parameter efficiency?

Here we present our results for 2 and 4 layer transformers trained on Fineweb-edu, with the same experimental settings as the main body of the paper: maximal update (μP) parameterization, context length of 50, and a fixed batch size of 100 sequences. The results are qualitatively similar to results presented in other cases. The main interesting point is that we find that for both 2 and 4 layer transformers, the mean exponent $\bar{\alpha}_D \approx 0.5$, which is larger than the case of SP, which had $\bar{\alpha}_D \approx 0.35$. This indicates that these settings are more parameter efficient, as the loss decreases more sharply with N . This is also reflected in the compute optimal exponents $(a, b) \approx (0.42, 0.58)$, which shows that the optimal parameter size need not grow as quickly with compute as in the case of standard parameterization; that is, compute optimal training is not at fixed token number per parameter. Since μP was designed to give $O(1)$ feature updates in the large width limit Yang and Hu (2021) it is plausible that it could be more parameter efficient for compute optimal training. It would be interesting to see if these results hold robustly at larger scales.

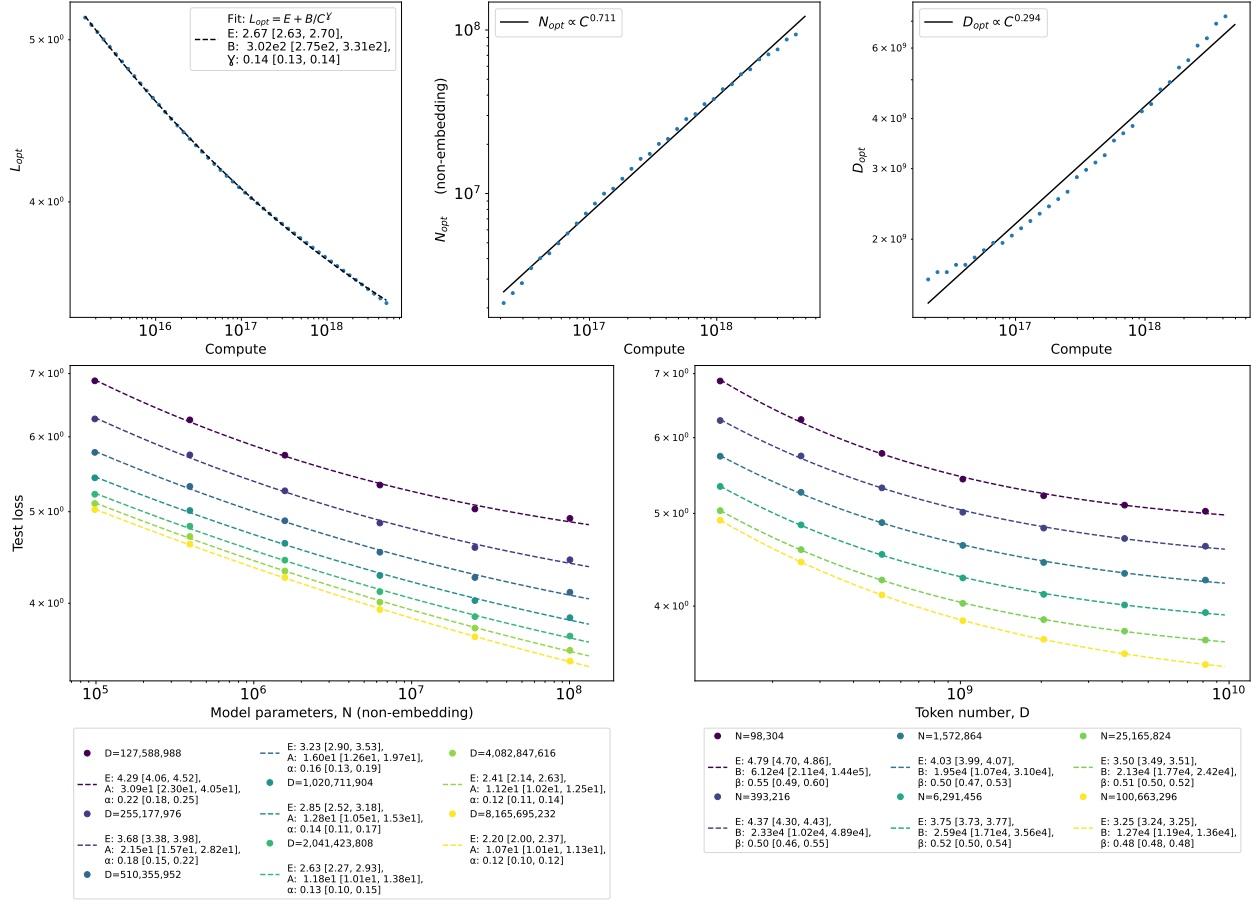


Figure 12 2 layer transformer trained on language with *SP*. Here N refers to non-embedding parameters, in contrast to the rest of the paper.

6 Additional related work

Transformers and random walks / Markov chains. (Perozzi et al., 2014; Shi and Cao, 2025; Makkuvu et al., 2025; Edelman et al., 2024) study the ability of neural networks to learn random walks or Markov processes, often focusing on model capability and learnability. Our work instead focuses on using random walks on graphs as a paradigm for understanding neural scaling laws.

Neural scaling laws Several works in addition to those referenced earlier also examine the origin of neural scaling laws. (Sharma and Kaplan, 2022; Bahri et al., 2021) show that the existence of a data manifold implies neural scaling laws. The data in our work consists of sequences of discrete tokens, which have no obvious data manifold, so such an explanation appears to be inapplicable.

Other mechanisms for neural scaling laws that have been studied include (Liu et al., 2025), which isolates “superposition” as an important underlying principle, and (Song et al., 2024) which proposes a resource-based theory. It would be interesting if these perspectives could be related to scaling laws we observed in the context of random walks. (Hutter, 2021) was an early paper suggesting that power laws in the data were responsible for “interesting” scaling laws (i.e. data exponents $\alpha \neq 0.5$ or 1) with respect to dataset size, although there is no neural network architecture and associated model parameter scaling law in Hutter’s model.

Scaling laws with μP (Dey et al., 2023) studied compute-optimal scaling in the case of fixed tokens-per-parameter, finding that μP gave $\sim 1\%$ better loss and more robust scaling laws. We are not aware of reports in the literature of the scaling law exponents for μP ; in this paper we find that μP is more parameter-efficient (larger $\overline{\alpha_D}$ and smaller a) than SP at relatively small scales.

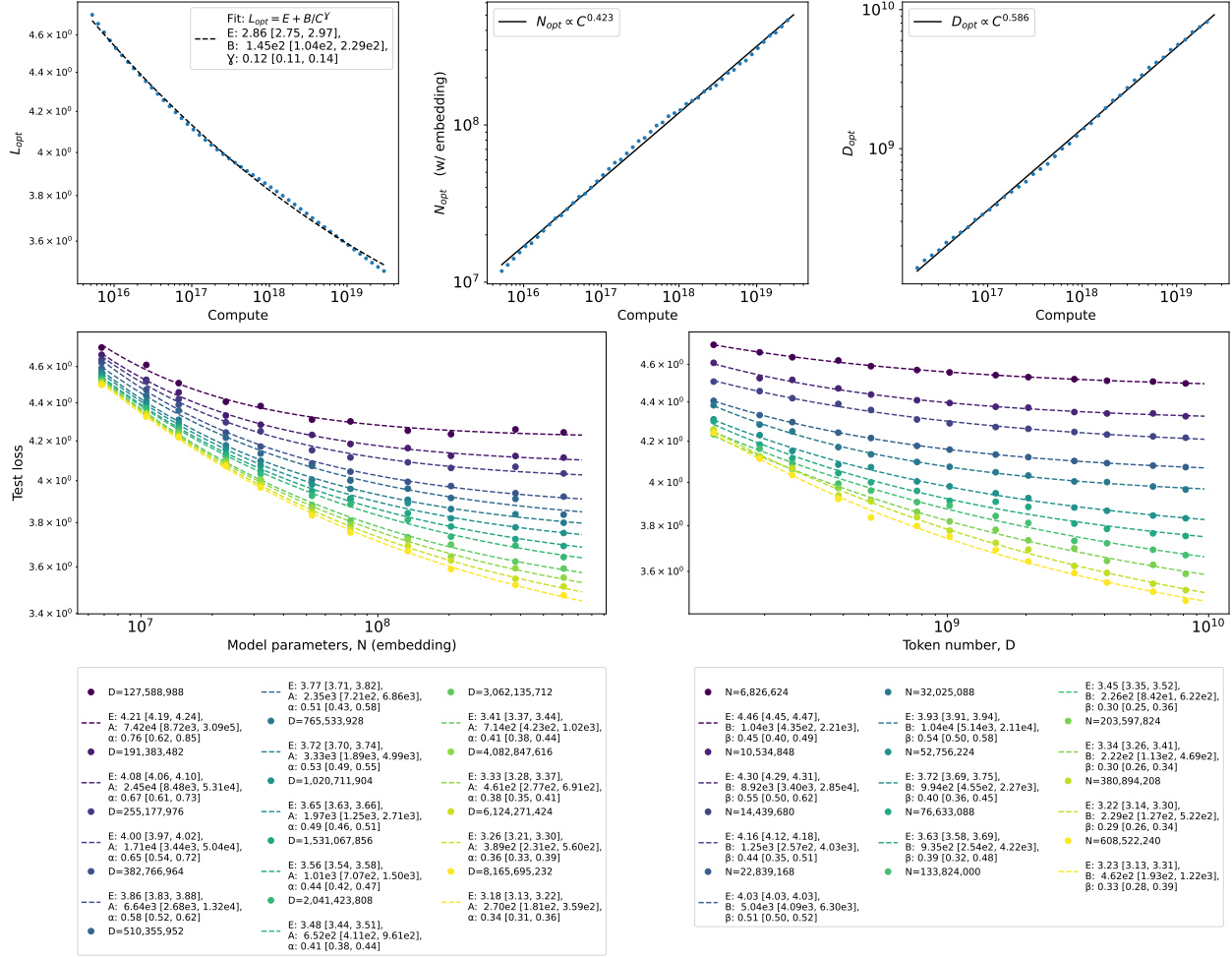


Figure 13 2 layer transformer trained on language (Fineweb-edu) with μP , context length 50, and batch size of 100 sequences. Mean exponent $\overline{\alpha_D} = 0.501$ with a standard deviation of 0.125. Mean exponent $\overline{\beta_N} = 0.408$ with standard deviation 0.093. Average MSE for $L(N)_D$ 1d power law fits is 1.19×10^{-4} , compared to 1.76×10^{-3} for the best exponential fits. Average MSE for $L(D)_N$ 1d power law fits is 9.05×10^{-5} , compared to 1.32×10^{-3} for the best exponential fits.

7 Discussion

We have demonstrated that neural scaling laws, as observed empirically in large language models, can also be observed in the simpler setting of Markov random walks on graphs. We have studied a wide variety of settings: (i) Erdős-Renyi graphs (1K nodes, 5K edges; 8K nodes, 50K edges; 50K nodes, 2M edges) with unbiased ($\kappa = 0$) and biased ($\kappa = 1$) random walks; (ii) scale free Barabási-Albert graphs (8K nodes, 50K edges); (iii) language bigram graphs (50K nodes, 33M edges). We have also demonstrated that one can consider datasets of monotonically increasing complexity, from language bigrams, TnL, to natural language data, and that one can track the mean scaling exponents as the complexity is increased, revealing a monotonic decrease in $\overline{\alpha_D}$.

Upon analyzing the scaling exponents, we see that most of them appear to the right of the $\overline{\alpha_D} = \overline{\beta_N}$ line in Fig. 2. With some small deviations, we generally have $\overline{\alpha_D} \gtrsim \overline{\beta_N}$, which suggests that the loss is limited more by data than by architectural capacity. This may be related to our setting of 1 epoch training, where the number of training steps is tied to the dataset size; it is possible that relaxing this would make the models more sample efficient and increase $\overline{\beta_N}$. It is also likely related to the fact that the setting of Markov random walks is too simple to be limited by architectural capacity. It would be interesting to find settings that are more limited by architectural capacity than by dataset size, so that $\overline{\beta_N} \gg \overline{\alpha_D}$; this would be expected in more

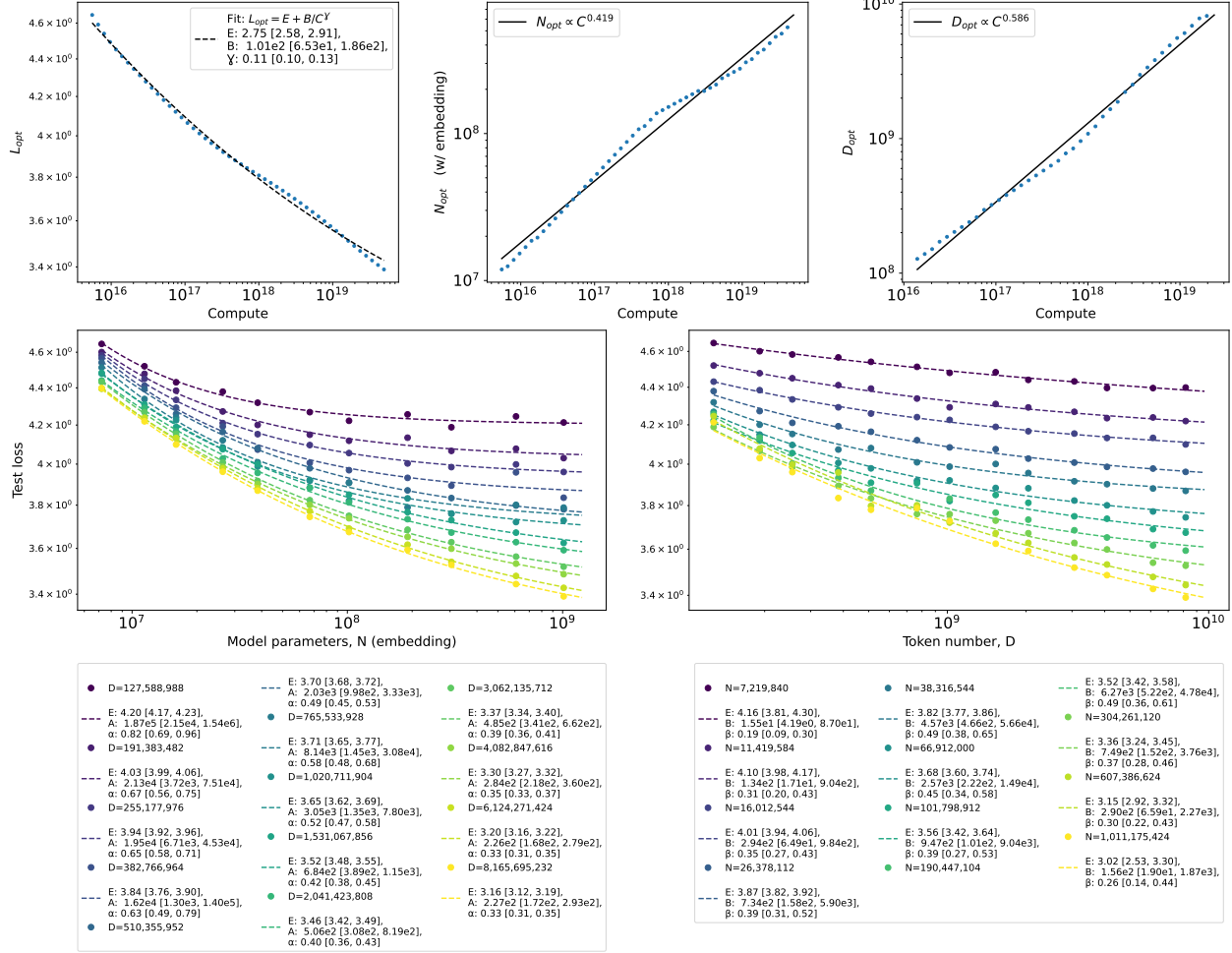


Figure 14 4 layer transformer trained on language (Fineweb-edu) with μP , context length 50, and batch size of 100 sequences. Mean exponent $\bar{\alpha}_D = 0.506$ with a standard deviation of 0.148. Mean exponent $\beta_N = 0.362$ with standard deviation 0.090. Average MSE for $L(N)_D$ 1d power law fits is 2.54×10^{-4} , compared to 2.30×10^{-3} for the best exponential fits. Average MSE for $L(D)_N$ 1d power law fits is 3.58×10^{-4} , compared to 2.04×10^{-3} for the best exponential fits.

complex datasets, where larger architectures are required to effectively learn, but where data is used more effectively, for example through multi-epoch training, data augmentation, synthetic data, self-play, and so on.

One of the key points of our paper, as exhibited by our results on unbiased random walks on ER graphs (Fig. 1), is that empirically neural scaling laws arise even when the data itself has no power law correlations. This calls for alternative explanations and a deeper understanding of neural scaling laws than have been provided so far in the literature. In the setting of one epoch training for a fixed dataset size D , the number of optimization steps is also fixed. As we increase N with fixed D , the scaling laws tell us that the model is able to reach a lower loss with the same number of training steps. Equivalently, the model is able to reach a given value of the loss with fewer steps. This suggests that the basin of low loss solutions is opening up in a particular way with model size, which allows gradient-based optimization to be more efficient. A potential path forward could be to study how the loss landscape is opening up with N and how this affects the gradients as a function of N during training.

In the kernel regression models referenced earlier, power law scaling in the loss arose from power laws in the features. While we have examples where the data has no power laws, it might be the case that power laws develop in the internal activations of the model, which then drive power law scaling in the loss. It would be interesting to further study these internal activations and see to what extent signatures of power laws arise.

While we found one method to dial the complexity of the data from bigrams to natural language via TnL, it would be interesting to develop alternative more controllable and systematic ways of interpolating in complexity between bigrams and natural language, such as through n -grams, skip n -grams, and hierarchical graphical structures. We leave a detailed study of these directions for future work.

Finally, we note that a difficult and important issue with scaling laws is to understand their robustness. First, the optimization algorithm is an important part of the story. All scaling laws observed empirically depend on a grid search over hyperparameters for a particular choice of optimization algorithm. Improving the optimization algorithm and the hyperparameter search will lower the loss $L(N, D)$; if different model sizes respond differently to these choices, the scaling laws could be altered substantially. In principle, a minimization over all possible optimization algorithms and hyperparameters separately at each N might remove the power law scaling in $L(N)_D$ altogether, because in many cases the shortcoming of smaller models is not expressivity but rather learnability.

Second, we observed, even in the case of Chinchilla’s data, that the parameters of the best fits were rather sensitive to the window over which the fitting was performed. As detailed in Appendix B, this is different from the bootstrap confidence intervals reported in our fits. A detailed sensitivity analysis is important for practitioners, and we leave it to for a separate careful study. Here we note that in addition to the exponents themselves, the sensitivity of the exponents is also an important quantity to characterize. Complex datasets like natural language might have more robust exponents than random walks; the former requires learning substantial interrelated hierarchical structures, while the former is more about learning a (large) table of transition probabilities. In our analysis, we saw some preliminary indications of this – our random graph results depended on careful hyperparameter grid searches, whereas our natural language results appeared to be more robust. We expect that further research along these lines will reveal additional insights into the origin of neural scaling laws.

8 Acknowledgments

We thank Newsha Ardalani, Yasaman Bahri, and Andrew Cohen for discussions and Rylan Schaeffer, Dan Roberts, and Cengiz Pehlevan for comments on the draft. MB thanks the Simons Collaboration on Physics of Learning and Neural Computation (SFI-MPS-POL-00012574-09) for support while at UMD.

A Experimental details

Transformer architectures. We train pre-normalization decoder-only transformer models (Vaswani et al., 2017; Radford et al., 2019) using rotary positional embedding (Black et al., 2022). We follow the rotary implementation available on Huggingface, with the default frequency base of 10,000 and with rotary dimension equal to the embedding dimension. The model vocabulary size is V , where V is the number of nodes in the graph. The models have 2 or 4 hidden layers, with embedding dimension ranging from $n_{\text{embd}} = 128$ to 4096. For each model, we set the number of attention heads to $\max(4, n_{\text{embd}}/64)$. No tokenizer is required, as each node in our graphs is treated as a distinct token with its own unique token ID. We tie the token embedding matrix and the output head weights (Press and Wolf, 2017).

Optimization. We initialize all models from scratch and pre-train them by minimizing the cross-entropy loss between the ground-truth data and predicted sequences. Model parameters are optimized using AdamW with a weight decay of 0.01 and a peak learning rate λ . We sweep λ over a grid of 14 values ranging from $5 \cdot 10^{-6}$ to 0.1. We use a learning rate schedule with a linear warmup for the first 2% of training steps, followed by cosine decay to 0. On each training step, we stack 100 independent random-walks into a tensor of shape $(100, T)$. We use the parameter initialization scheme and μP implementation from the nanoGPT-muP repository (Kalra, 2025); we found that μP helped mitigate training instabilities across the sweep of learning rates for our random walk experiments. For each hyperparameter configuration, we train 3 models with different random initialization seeds and we report the best test loss performance.

Data generation. We introduce synthetic random-walk datasets. We generate sequences using the following procedure:

- For a desired sequence length T (generally 50 or 100), we start from a weighted transition matrix W_{uv} and an initial-node distribution M_u where $\sum_v W_{uv} = 1$ for every node u and $\sum_u M_u = 1$. W_{uv} is the probability of moving from node u to node v in one step and M_u is the probability of choosing node u as the starting point.
- We sample the first node of each sequence from M_u .
- We then sample the remaining $T - 1$ nodes by repeatedly drawing the next node v according to W_{uv} , where u is the current node.
- These walks may revisit nodes and traverse the same edge multiple times (i.e. node and edge repetition is allowed).

For Erdős-Renyi or Barabási-Albert graphs, we first create a graph \mathcal{G} with V nodes and E edges, yielding a binary symmetric adjacency matrix A_{uv} . For biased walks, we sample W_{uv}^{init} from a power-law distribution $\Pr(W_{uv}^{init} = k) \propto k^{-\kappa}$, for $k \in [k_{\min}, k_{\max}]$ whenever $A_{uv} = 1$ and set $W_{uv}^{init} = 0$ otherwise. For unbiased walks, we let $W_{uv}^{init} = A_{uv}$.

For bigram graphs, we first tokenize the Fineweb-edu-10B dataset (Penedo et al., 2024) using the GPT-2 tokenizer (Radford et al., 2019), which has a vocabulary of size 50,257. This tokenized dataset has approximately 130M unique bigrams. We remove all bigrams that appear 5 times or fewer, leaving around 33M unique bigrams. Let C_{uv} denote the number of occurrences of the bigram (u, v) in the filtered corpus and set $W_{uv}^{init} = C_{uv}$.

Finally, we define

$$W_{uv} = \frac{W_{uv}^{init}}{\sum_j W_{uj}^{init}} \quad \text{and} \quad M_u = \frac{\sum_j W_{uj}^{init}}{\sum_{i,j} W_{ij}^{init}}.$$

For T1L, T2L and T4L, we train a n -layer transformer (respectively $n = 1, 2, 4$) with an embedding dimension of 4096 and a vocabulary size of 50,257 on the Fineweb-edu-10B dataset (Penedo et al., 2024). We train with a context length of 50, batch size of 100 and choose the learning rate λ that minimizes the training loss. After training, we sample random sequences from the model using temperature 1.

All natural language experiments are done with Fineweb-edu.

B Fitting scaling laws

B.1 $L(N)_D$ and $L(D)_N$ fits

To fit $L(D)_N$ and $L(N)_D$, we fit the power law

$$y(x) = E + B x^{-\beta} \quad (\beta > 0)$$

by minimizing a Huber-robust least-squares objective with cutoff δ . Specifically, for residuals $r_i = y(x_i; \theta) - y_i$, we minimize $\sum_i \rho_\delta(r_i)$, where

$$\rho_\delta(r) = \begin{cases} \frac{1}{2}r^2, & |r| \leq \delta, \\ \delta(|r| - \frac{1}{2}\delta), & |r| > \delta, \end{cases}$$

so errors smaller than δ are treated quadratically while larger errors are penalized approximately linearly (down-weighting outliers). We set $\delta = 1.4826\text{MAD}(y)$, where $\text{MAD}(y) = \text{median}(|y - \text{median}(y)|)$ is the median absolute deviation, and provides an estimate for an appropriate scale of δ . (If y is pure Gaussian noise, this reduces to $\delta = \sigma$, the standard deviation of the Gaussian noise; on the other hand, if y is dominated by signal and noise is small, δ is large and the fit reduces to ordinary least squares). We use a fallback $\delta = 0.1\text{std}(y)$ if the median absolute deviation is zero. For numerical stability we reparameterize as

$$y(x) = E + A \left(\frac{x}{x_0} \right)^{-\beta}, \quad x_0 = \text{median}(x), \quad A > 0,$$

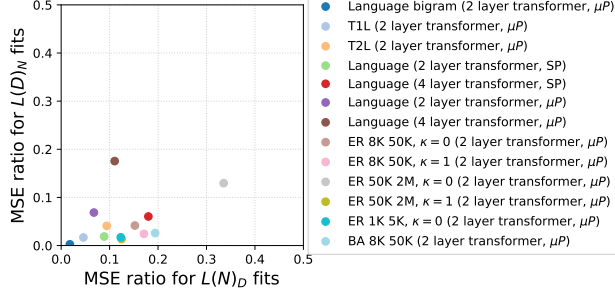


Figure 15 Ratio of the mean-squared error between the best power-law and the best exponential ($y = a + be^{-cx}$) fits, in order to validate the power-law scaling hypothesis. The power law fits for $L(D)_N$ are extremely good. The ones for $L(N)_D$ are generally not as clean, but it is unambiguous that the power law form gives a substantially better fit. Biased random walks with power-law weights give clearer power-laws than unbiased random walks for Erdős-Renyi graphs.

optimize over $(E, \log A, \log \beta)$ with bounds $\beta \in [\beta_{\min}, \beta_{\max}]$, and then report $B = Ax_0^\beta$. The bounded nonlinear optimization (trust-region reflective algorithm) is run from 40 initializations: E_0 is chosen from y -quantiles, with (A_0, β_0) obtained from an approximate log-linear fit of $\log(y - E_0)$ versus $\log(x/x_0)$ on points where $y - E_0 > 0$, plus additional random starts; we keep the solution with the smallest final Huber objective.

For all of our $L(N)_D$ and $L(D)_N$ fits, we compare the quality of the power law fit to the quality of the best exponential fit, $y = a + be^{-cx}$, by examining the MSEs of the power law and exponential fits. The ratios of the power law and exponential MSEs for the datasets studied in this paper are shown in Fig. 15. This demonstrates that the power law fits for $L(D)_N$ are extremely good (a factor of 50-100x better than the best exponential fits). The power law fits for $L(N)_D$ are also good; with one exception, they are between 5-100x better than the best exponential fits.

B.2 Confidence intervals

In our fits we report 95% confidence intervals (shown in square brackets in the figure legends) for $\theta = (E, B, \beta)$ in the power law $y(x) = E + Bx^{-\beta}$ using a fixed- x wild bootstrap with BCa correction. After obtaining the robust point estimate $\hat{\theta}$ and fitted values $\hat{y}_i = \hat{E} + \hat{B}x_i^{-\hat{\beta}}$, we form residuals $r_i = y_i - \hat{y}_i$. For each bootstrap replicate $b = 1, \dots, N_{\text{boot}}$, we generate

$$y_i^{*(b)} = \hat{y}_i + \varepsilon_i^{(b)} r_i, \quad (9)$$

with i.i.d. weights $\varepsilon_i^{(b)} = \pm 1$ satisfying $\mathbb{E}[\varepsilon] = 0$ and $\text{Var}(\varepsilon) = 1$. We refit the model to $\{(x_i, y_i^{*(b)})\}$ using the same Huber objective and the same cutoff δ as in the base fit, warm-starting the optimizer from the base solution; failed refits are discarded.

For each scalar parameter $t \in \{E, B, \beta\}$ we obtain bootstrap draws $\{\hat{t}^{*(b)}\}_{b=1}^{N_{\text{boot}}}$ and use BCa (bias-corrected and accelerated) intervals. The *bias-correction* term is

$$z_0 = \Phi^{-1} \left(\frac{\#\{\hat{t}^{*(b)} < \hat{t}\} + \frac{1}{2} \#\{\hat{t}^{*(b)} = \hat{t}\}}{N_{\text{boot}}} \right), \quad (10)$$

which measures how the bootstrap distribution is shifted relative to the point estimate \hat{t} (here Φ is the standard normal CDF). The *acceleration* term a is estimated via a leave-one-out jackknife: for each $i = 1, \dots, n$ we refit the model on the dataset with observation i removed, yielding jackknife estimates $t_{(i)}$ and mean $\bar{t}_{(\cdot)} = \frac{1}{n} \sum_i t_{(i)}$. We then set

$$a = \frac{\sum_{i=1}^n (\bar{t}_{(\cdot)} - t_{(i)})^3}{6 \left[\sum_{i=1}^n (\bar{t}_{(\cdot)} - t_{(i)})^2 \right]^{3/2}}. \quad (11)$$

Given nominal quantiles $\alpha/2$ and $1 - \alpha/2$ (with $\alpha = 0.05$ for 95% CIs), we compute adjusted quantile levels

$$\alpha_{\text{BCa}}(q) = \Phi\left(z_0 + \frac{z_0 + \Phi^{-1}(q)}{1 - a(z_0 + \Phi^{-1}(q))}\right), \quad (12)$$

and take the endpoints as the empirical $\alpha_{\text{BCa}}(\alpha/2)$ and $\alpha_{\text{BCa}}(1 - \alpha/2)$ quantiles of $\{\hat{t}^{*(b)}\}$. We also report bootstrap standard errors as the sample standard deviation of $\{\hat{t}^{*(b)}\}$.

For the $L(D)_N$ and $L(N)_D$, we use $N_{\text{boot}} = 4000$ bootstrap samples.

B.3 Fitting $L(N, D)$

We compare three different methods for fitting a two-dimensional function $L(N, D)$, which allows determination of compute optimal scaling laws. In all cases below, we use the Huber loss, with $\delta = 1 \times 10^{-3}$ to match the setting in (Hoffmann et al., 2022; Besiroglu et al., 2024).

Fitting with 2d Chinchilla formula. We fit to Eq. 3 following the methodology of (Hoffmann et al., 2022). We use the code and data from the github repository of (Besiroglu et al., 2024).

Neural network regression with 3-layer FCN. We fit $L(N, D)$ with a 3-layer fully connected neural network containing linear layers of dimension $2 \times n$, $n \times n$, and $n \times 1$ and GeLU activations. For fitting the Chinchilla data, we used a width $n = 512$; for the rest of the fits we use $n = 256$. The model achieving the best loss is used, within 5000 epochs of AdamW (weight decay $1e-4$) or until the loss has stopped improving by more than $1e-6$ for more than 200 steps.

Kernel ridge regression. We fit $L(N, D)$ with the ANOVA-style RBF kernel

$$k(x, x') = w_n \exp\left(-\frac{(n-n')^2}{2\ell_n^2}\right) + w_d \exp\left(-\frac{(d-d')^2}{2\ell_d^2}\right) + w_{nd} \exp\left(-\frac{(n-n')^2 + (d-d')^2}{2\ell_{nd}^2}\right),$$

with nonnegative amplitudes $w_{\{\cdot\}}$ and length-scales $\ell_{\{\cdot\}}$, where $x = (n, d) = (\log_{10} N, \log_{10} D)$. This kernel induces the function decomposition $f(x) = f_n(n) + f_d(d) + f_{nd}(n, d)$, recovering a standard RBF when $w_n = w_d = 0$. We set $w_{\{\cdot\}} = \ell_{\{\cdot\}} = 1$, although in principle a hyperparameter search can be carried out. The inputs x are centered and normalized and the outputs are centered. The regression minimizes the objective $\sum_i \rho_\delta(y_i - f_i) + (\lambda/2)\alpha^T K \alpha$, with $f = K\alpha$, where ρ_δ is the Huber loss. This is solved by iteratively reweighted least squares (IRLS) with per-sample weights $w_i = 1$ if $|r_i| \leq \delta$ and $w_i = \delta/|r_i|$ otherwise, and a linear system at each step: $(WK + \lambda I)\alpha = Wy_c$

B.4 Fitting compute optimal scaling laws, $L_{\text{opt}}, N_{\text{opt}}, D_{\text{opt}}$

We use the fits $\hat{L}(N, D)$ obtained using the neural network regression approach. We pick a grid of 50 or 100 points between the minimum and maximum values of N in our raw data, and similarly for D . We then determine the compute optimal loss in two ways, by $\min_N \hat{L}(N, C/6N)$ and $\min_D \hat{L}(C/6D, D)$. For a sufficiently dense grid and smooth enough fit \hat{L} , these two should coincide. This gives us an estimate of the compute optimal loss $L_{\text{opt}}(C)$. We fit $L_{\text{opt}}(C)$ to the power law form using the same methodology we used for $L(D)_N$ and $L(N)_D$, although we instead use 200 bootstrap samples for the confidence intervals since we observed the confidence intervals are already stable for those values of N_{boot} .

Next, from the fit $\hat{L}(N, D)$ over the grid described above, we obtain $N_{\text{opt}}(C)$ and $D_{\text{opt}}(C)$ using Eq. 6. We fit then do a standard linear regression to fit $\log N_{\text{opt}}(C)$ and $\log D_{\text{opt}}(C)$ to a line to extract the compute optimal exponents a and b .

In almost cases, we have to clip by hand the lower and upper values of C . One reason is that near the boundaries $C_{\text{min}} = 6N_{\text{min}}D_{\text{min}}$ and $C_{\text{max}} = 6N_{\text{max}}D_{\text{max}}$, the fit is less accurate and so $L_{\text{opt}}(C)$, N_{opt} , and D_{opt} exhibit spurious behavior in these limits. Another reason is that in some cases, N_{opt} and D_{opt} are beyond the grid for N, D we have sampled.

We observed in practice that the neural network regression usually appears to give more sensible results for the compute optimal curves as compared with the kernel regression approach, so in all of our figures we report results using the neural network regression. We eschew the 2d Chinchilla fit for the neural network regression

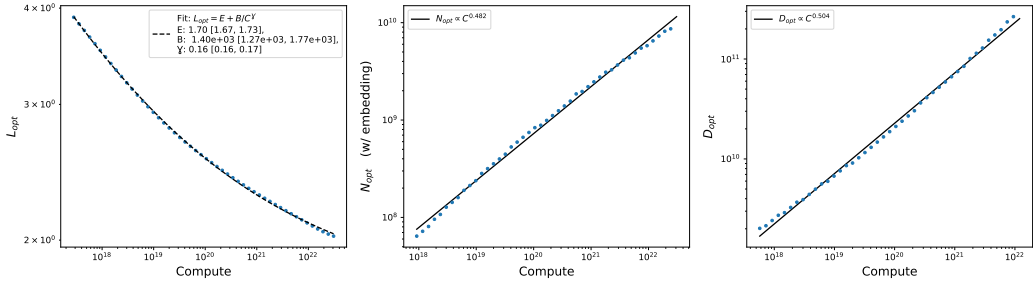


Figure 16 Compute optimal scaling laws obtained using the neural network fit for $L(N, D)$.

approach because it gives significantly better MSEs for the fits, as shown in Figs. 10, 17, 18, and explained in the main text.

In nearly all cases, we found that the parameters of the fits for the scaling laws are sensitive to the window chosen for the fits. In principle the confidence intervals should also include a sensitivity analysis with respect to the window of the fit; we leave a detailed such analysis, which is of particularly important in for natural language data, for future work.

Fig. 16 demonstrates the neural network regression approach introduced above for obtaining compute optimal scaling curves for the raw Chinchilla data that we reanalyzed in Sec. 5.2. As described in the main text, the exponents are close to those obtained via other methods in (Hoffmann et al., 2022; Besiroglu et al., 2024).

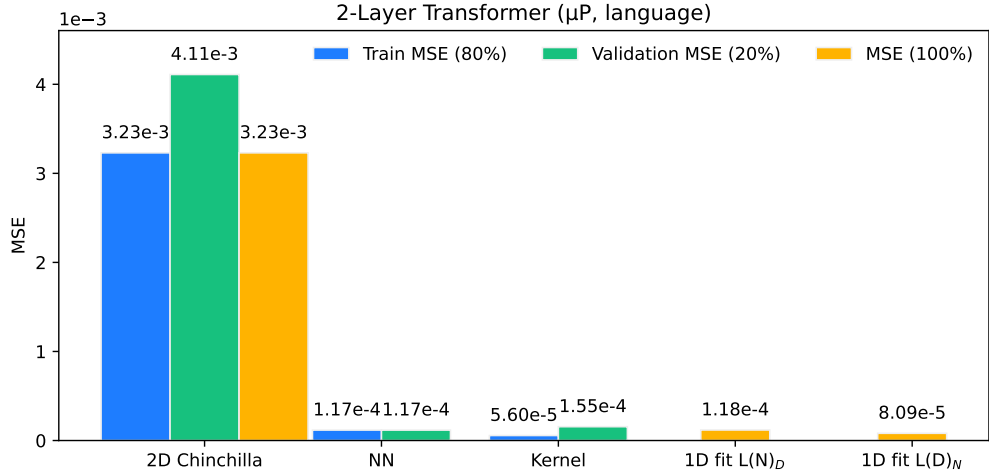


Figure 17 The 2d Chinchilla fit is around 30 – 40× worse than the NN and kernel fits. N = embedding parameters. Non-embedding is similar.

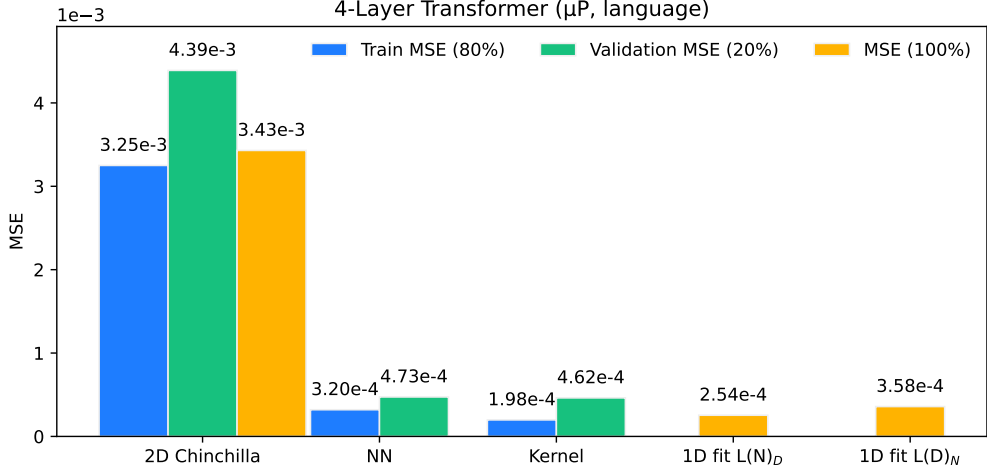


Figure 18 N = embedding parameters. Non-embedding is similar. 2d Chinchilla fit yields the parameters $A = 1838$, $B = 677$, $E = 3.342$, $\alpha = 0.484$, $\beta = 0.378$

C Sample error baseline

Consider the problem of estimating a probability distribution π over a finite sample space V . Given a dataset of D samples, consider the counting estimate

$$\hat{\pi}_a = \frac{n_a}{D}, \quad (13)$$

where n_a is the number of times $a \in V$ appears in the dataset. Here we derive the data scaling laws for this counting model for cross-entropy and MSE losses, which provides a baseline against which to compare the random walk scaling law results. Note that this model was also studied in the Appendix of (Hestness et al., 2017) using a loss based on L1 norm, where a $1/\sqrt{D}$ scaling was computed; here we extend the analysis to MSE and cross-entropy loss, which gives a $1/D$ scaling law.

If we let X be a random variable with V outcomes and probability distribution π , then $\hat{\pi}_a$ is the sample mean of the indicator function $I_a = \text{Ind}(X = a)$. The mean and variance of $\hat{\pi}_a$ are given by:

$$\begin{aligned} \mathbb{E}[\hat{\pi}_a] &= \pi_a \\ \text{Var}[\hat{\pi}_a] &= \mathbb{E}[(\hat{\pi}_a - \pi_a)^2] = \frac{1}{D}\pi_a(1 - \pi_a) \\ \mathbb{E}[(\hat{\pi}_a - \pi_a)^3] &= \mathbb{E}[\hat{\pi}_a^3 - 3\hat{\pi}_a^2\pi_a + 3\hat{\pi}_a\pi_a^2 - \pi_a^3] = \frac{1}{D^2}\pi_a(2\pi_a - 1)(\pi_a - 1) \end{aligned} \quad (14)$$

Let us consider both mean-squared error and cross-entropy loss in this situation. By the central limit theorem, since $\hat{\pi}_a$ is the average over D i.i.d. binary random variables, its distribution in the large D limit is given by a Gaussian:

$$\hat{\pi}_a \sim \mathcal{N}(\pi_a, \frac{\sigma_a^2}{D}), \quad (15)$$

where $\sigma^2 = \pi_a(1 - \pi_a)$ is the variance of I_a .

C.1 Mean squared error

$$L_{MSE} = \frac{1}{|V|} \sum_{a \in V} (\pi_a - \hat{\pi}_a)^2. \quad (16)$$

Its expected value is

$$\begin{aligned}
\mathbb{E}[L_{MSE}] &= \frac{1}{|V|} \sum_{a \in V} \mathbb{E}[(\hat{\pi}_a - \mathbb{E}[\hat{\pi}_a])^2] \\
&= \frac{1}{|V|} \sum_{a \in V} \text{Var}[\hat{\pi}_a] \\
&= \frac{1}{D} \frac{1}{|V|} \sum_{a \in V} \pi_a(1 - \pi_a)
\end{aligned} \tag{17}$$

C.2 Cross-entropy loss

The cross-entropy loss is ²

$$L_{CSE} = - \sum_{a \in V} \pi_a \log \hat{\pi}_a \tag{18}$$

The expected value is:

$$\begin{aligned}
\mathbb{E}[L_{CSE}] &= - \sum_{a \in V} \pi_a \mathbb{E}[\log \pi_a (1 + \frac{(\hat{\pi}_a - \pi_a)}{\pi_a})] \\
&= S_\pi - \sum_{a \in V} \pi_a \sum_{n=1}^{\infty} \frac{(-1)^{(n+1)}}{n} \pi_a^{-n} \mathbb{E}[(\hat{\pi}_a - \pi_a)^n],
\end{aligned} \tag{19}$$

where $S_\pi = - \sum_{a \in V} \pi_a \log \pi_a$ is the entropy of π . Evaluating the expectation values for $\hat{\pi}_a$ gives:

$$\begin{aligned}
\mathbb{E}[L_{CSE}] &= S_\pi + \frac{1}{D} \frac{1}{2} \sum_{a \in V} (1 - \pi_a) - \frac{1}{3} \sum_a \frac{1}{\pi_a^2} \mathbb{E}[(\hat{\pi}_a - \pi_a)^3] + \dots \\
&= S_\pi + \frac{|V| - 1}{2D} - \frac{1}{3D^2} \sum_a \frac{(2\pi_a - 1)(\pi_a - 1)}{\pi_a} + O(1/D^3) \\
&= S_\pi + \frac{|V| - 1}{2D} + \frac{1}{D^2} (|V| - \frac{2}{3} - \frac{1}{3} \sum_a 1/\pi_a) + O(1/D^3)
\end{aligned} \tag{20}$$

We see that in both cases, we get an exponent $\beta = 1$ for the asymptotic power-law scaling of the population loss. These results can easily be verified empirically.

C.3 Application to graph random walk

Let us consider applying the above to the graph random walk problem. There, for each node v , we want to learn a probability distribution $p(u|v)$ from the sequences. The node v itself appears with probability $p(v)$. Therefore if we have a dataset of D tokens, approximately $p(v)D$ of them will be v . So our effective dataset size for each node is $D_{\text{eff},v}$, which is equal to $p(v)D$ in the large D limit. For each node v we have a counting estimate $\hat{p}(u|v)$, leading to a cross-entropy loss for each node:

$$\mathbb{E}[L_{CSE,v}] = S_{p(\cdot|v)} + \frac{\deg(v) - 1}{2D_{\text{eff},v}} + O(1/D^2). \tag{21}$$

The total cross-entropy loss, averaging over all nodes is then:

$$\begin{aligned}
\mathbb{E}[L_{CSE}] &= \sum_v p(v) \mathbb{E}[L_{CSE,v}] = \sum_v p(v) S_{p(\cdot|v)} + \sum_v \frac{\deg(v) - 1}{2D} + O(1/D^2) \\
&= \langle S_{p(\cdot|v)} \rangle + \frac{2E - n}{2D} + O(1/D^2)
\end{aligned} \tag{22}$$

For the unbiased random walk, $p(u|v) = A_{uv}/\deg(v)$ and the stationary distribution on nodes is $p(v) = \deg(v)/2E$.

²Note that for this to be well-defined for finite samples, where $\hat{\pi}_a$ might be zero even when $\pi_a \neq 0$, we must assume some smoothing, which we keep implicit.

D Additional scaling law results

D.1 Number of bigrams vs. count: most bigrams appear only a few times

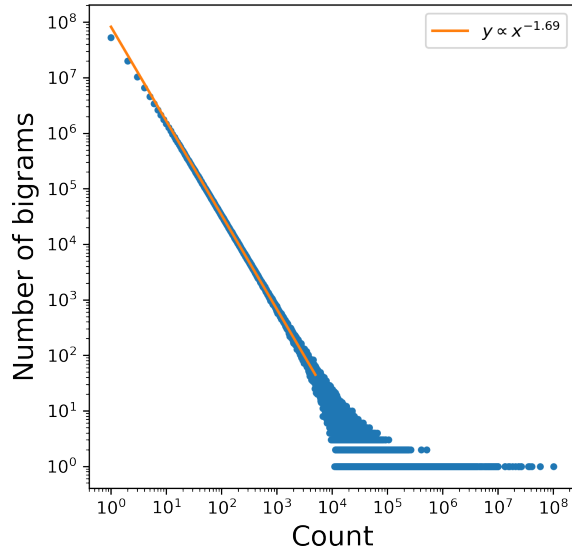


Figure 19 Number of bigrams that appear a given number (Count) of times, showing perfect linear fit on log-log scale. This plots demonstrates how almost all (over 100 million) bigrams appear only a handful of times.

D.2 4 layer transformer trained on language (Fineweb-edu) with Standard Parameterization

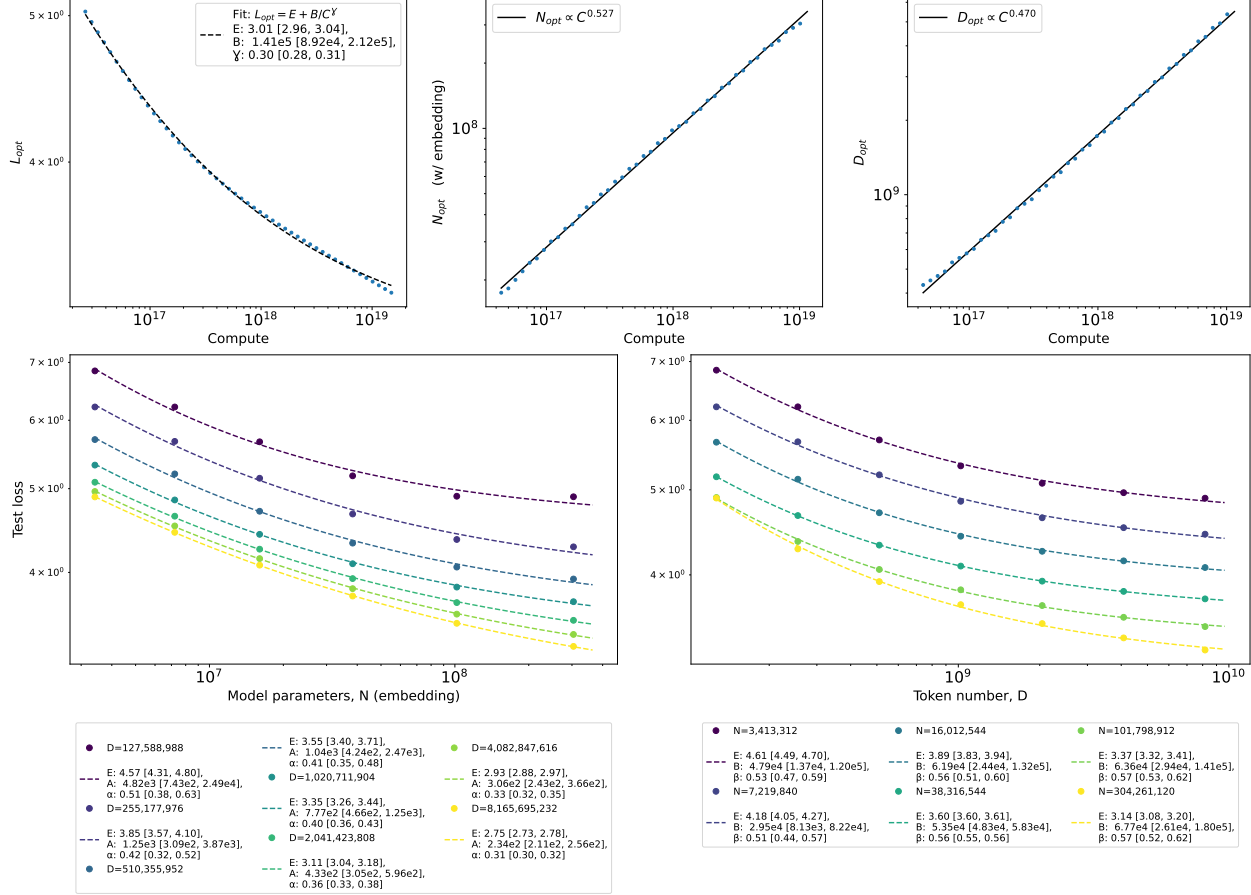


Figure 20 4 layer transformer on language (Fineweb-edu) with Standard Parameterization. Mean exponent $\overline{\alpha_D} = 0.391$ with standard deviation 0.060. Mean exponent $\beta_N = 0.550$ with standard deviation 0.020. Average MSE for $L(N)_D$ 1d power law fits is 1.28×10^{-3} , as compared with 7.11×10^{-3} for best exponential fit. Average MSE for $L(D)_N$ 1d power law fits is 4.51×10^{-4} , compared to 7.47×10^{-3} for best exponential fit.

D.3 Barabási-Albert graph with 8K nodes, 50K edges

Fig. 21 shows our results for a scale-free Barabási-Albert graph.

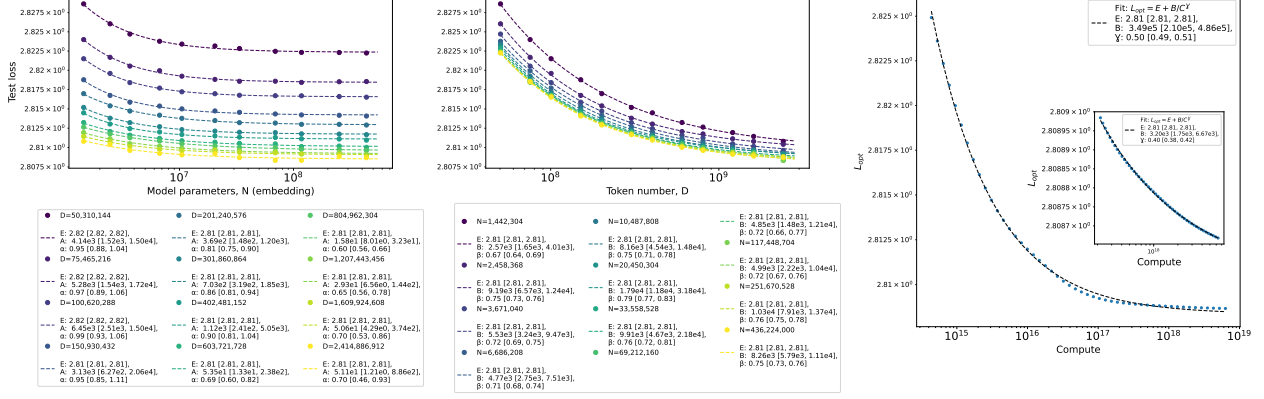


Figure 21 Results for Barabasi-Albert graph with 8,192 nodes. Mean $\overline{\alpha_D} = 0.815$ with standard deviation 0.133. Mean $\beta_N = 0.735$ with standard deviation 0.031. Average MSE for $L(N)_D$ 1d power law fits: 1.22×10^{-8} compared with 6.29×10^{-8} for best exponential fit. Average MSE for $L(D)_N$ 1d power law fits: 1.32×10^{-8} compared with 5.07×10^{-7} for best exponential fit.

D.4 Erdös-Renyi graphs with 50K nodes and 2M edges, $\kappa = 0, 1$

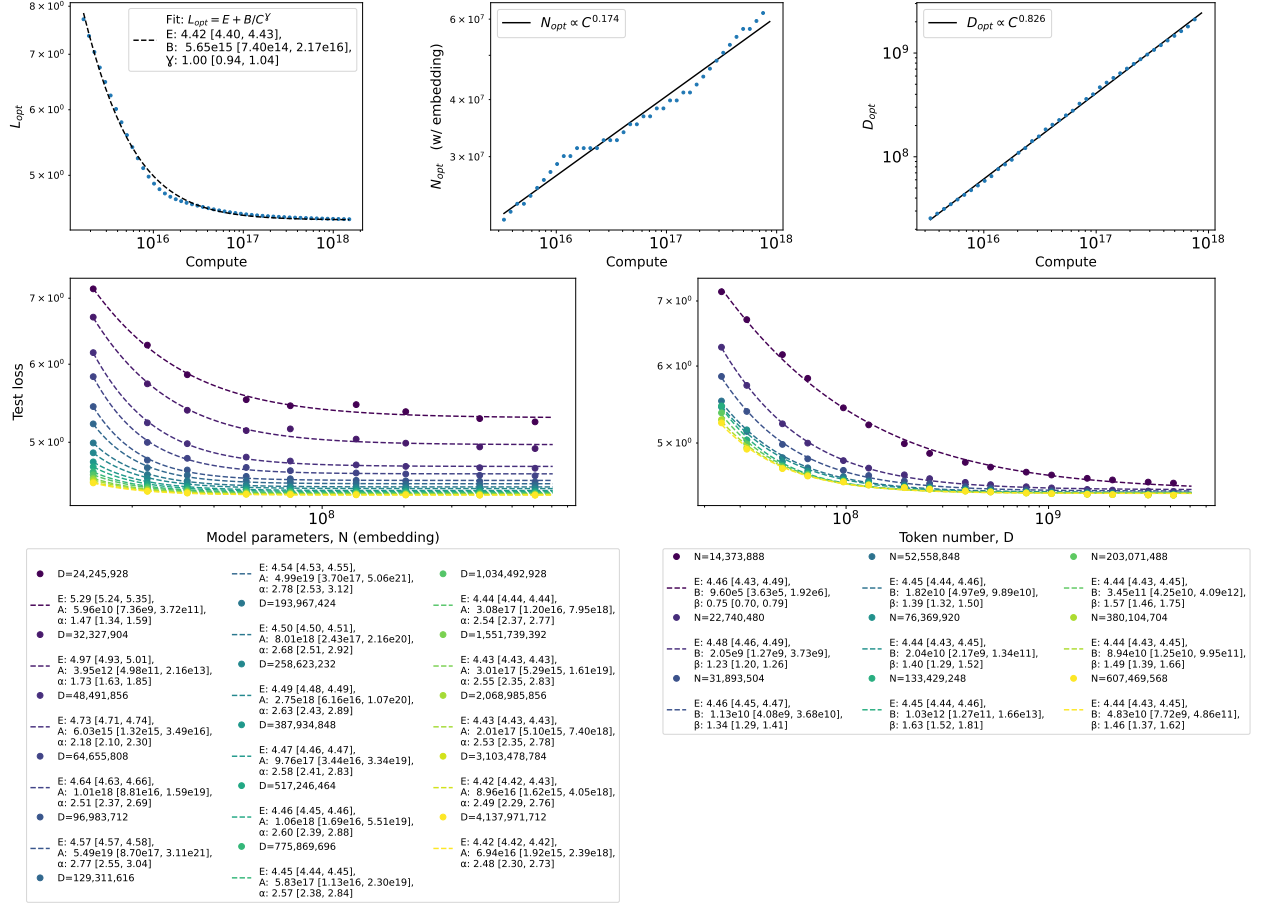


Figure 22 Results for Erdos-Renyi graph with 50,000 nodes and 2 million edges, with unbiased sampling $\kappa = 0$. Mean $\alpha = 2.443$, with standard deviation of 0.348. Mean $\beta = 1.361$ with standard deviation = 0.244. Average MSE for $L(N)_D$ 1d power law fits is 2.76×10^{-4} as compared with 8.23×10^{-4} for the best exponential fit. Average MSE for the $L(D)_N$ 1d power law fits is 3.99×10^{-4} , and best exponential fit gives 3.08×10^{-3} .

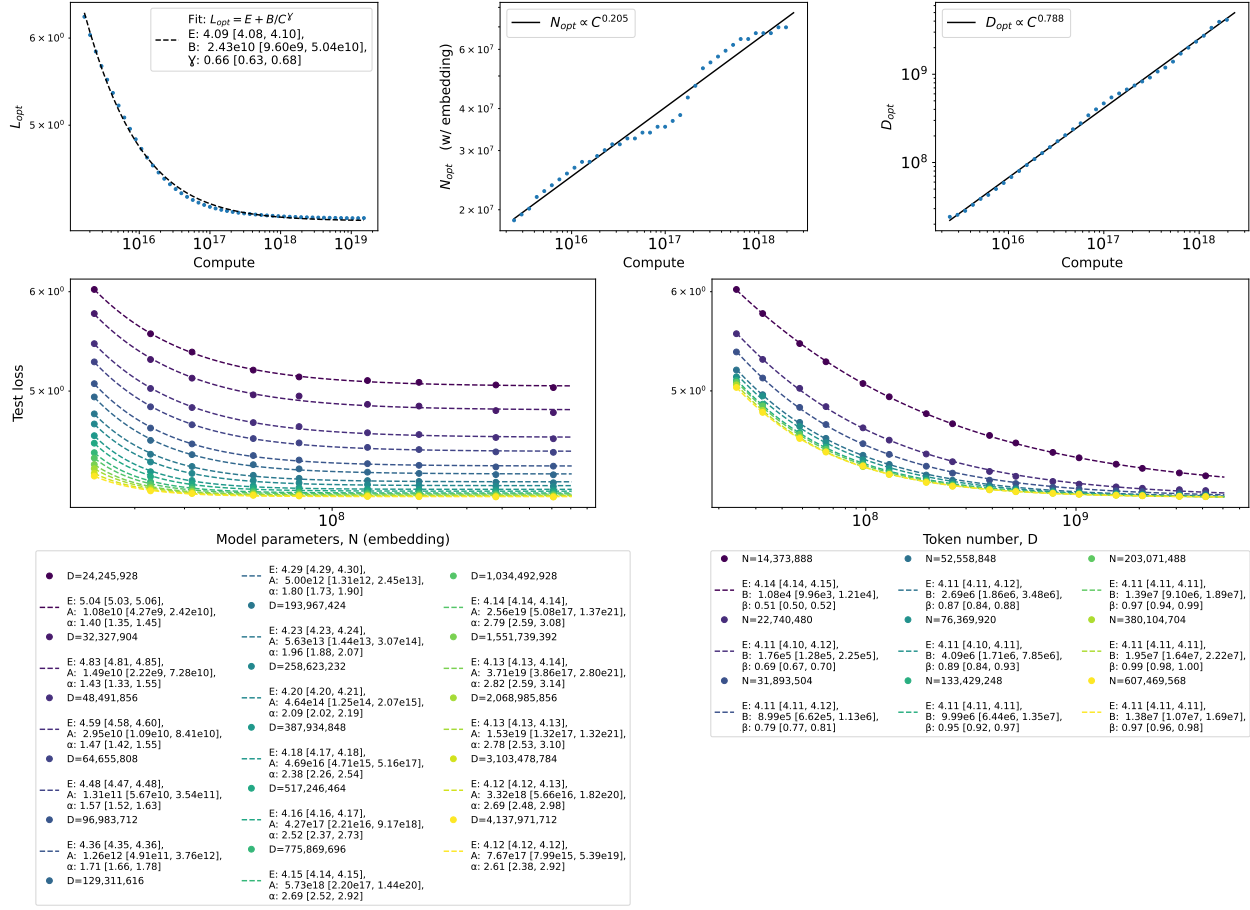


Figure 23 Results for Erdos-Renyi graph with 50,000 nodes and 2 million edges, with biased sampling $\kappa = 1$. Mean $\alpha = 2.169$ with standard deviation 0.529. Mean $\beta = 0.847$ with standard deviation 0.151. Average MSE for $L(N)_D$ 1d power law fits: 5.30×10^{-5} , compared with 4.25×10^{-4} for best exponential fit. Average MSE for $L(D)_N$ 1d power law fits: 4.05×10^{-5} , compared with 2.99×10^{-3} for best exponential fit.

References

Eduardo G Altmann and Martin Gerlach. Statistical laws in linguistics. In *Creativity and universality in language*, pages 7–26. Springer, 2016.

Yasaman Bahri, Ethan Dyer, Jaehoon Lee, Jared Kaplan, and Utkarsh Sharma. Explaining neural scaling laws. *arXiv preprint arXiv:2102.06701*, 2021. <https://arxiv.org/abs/2102.06701>.

Albert-László Barabási and Réka Albert. Emergence of scaling in random networks. *science*, 286(5439):509–512, 1999.

Tamay Besiroglu, Ege Erdil, Matthew Barnett, and Josh You. Chinchilla scaling: A replication attempt, 2024. <https://arxiv.org/abs/2404.10102>.

Maciej Besta, Nils Blach, Ales Kubicek, Robert Gerstenberger, Michal Podstawski, Lukas Gianinazzi, Joanna Gajda, Tomasz Lehmann, Hubert Niewiadomski, Piotr Nyczek, and Torsten Hoefer. Graph of thoughts: Solving elaborate problems with large language models. *Proceedings of the AAAI Conference on Artificial Intelligence*, 38(16):17682–17690, March 2024. ISSN 2159-5399. doi: 10.1609/aaai.v38i16.29720. <http://dx.doi.org/10.1609/aaai.v38i16.29720>.

Akshita Bhagia, Jiacheng Liu, Alexander Wettig, David Heineman, Oyvind Tafjord, Ananya Harsh Jha, Luca Soldaini, Noah A. Smith, Dirk Groeneveld, Pang Wei Koh, Jesse Dodge, and Hannaneh Hajishirzi. Establishing task scaling laws via compute-efficient model ladders, 2025. <https://arxiv.org/abs/2412.04403>.

Stella Biderman, Hailey Schoelkopf, Quentin Gregory Anthony, Herbie Bradley, Kyle O’Brien, Eric Hallahan, Mohammad Aflah Khan, Shivanshu Purohit, USVSN Sai Prashanth, Edward Raff, et al. Pythia: A suite for analyzing large language models across training and scaling. In *International Conference on Machine Learning*, pages 2397–2430. PMLR, 2023.

Sidney Black, Stella Biderman, Eric Hallahan, Quentin Anthony, Leo Gao, Laurence Golding, Horace He, Connor Leahy, Kyle McDonell, Jason Phang, et al. Gpt-neox-20b: An open-source autoregressive language model. In *Proceedings of BigScience Episode# 5—Workshop on Challenges & Perspectives in Creating Large Language Models*, pages 95–136, 2022.

Blake Bordelon, Abdulkadir Canatar, and Cengiz Pehlevan. Spectrum dependent learning curves in kernel regression and wide neural networks. In Hal Daumé III and Aarti Singh, editors, *Proceedings of the 37th International Conference on Machine Learning*, volume 119 of *Proceedings of Machine Learning Research*, pages 1024–1034. PMLR, 13–18 Jul 2020. <https://proceedings.mlr.press/v119/bordelon20a.html>.

Blake Bordelon, Alexander Atanasov, and Cengiz Pehlevan. A dynamical model of neural scaling laws. In *Proceedings of the 41st International Conference on Machine Learning (ICML)*, volume 235 of *Proceedings of Machine Learning Research*, pages 4345–4382. PMLR, 2024. <https://proceedings.mlr.press/v235/bordelon24a.html>.

Tom Brown, Benjamin Mann, Nick Ryder, Melanie Subbiah, Jared D Kaplan, Prafulla Dhariwal, Arvind Neelakantan, Pranav Shyam, Girish Sastry, Amanda Askell, et al. Language models are few-shot learners. *Advances in neural information processing systems*, 33:1877–1901, 2020.

Francesco Cagnetta, Leonardo Petrini, Umberto M Tomasini, Alessandro Favero, and Matthieu Wyart. How deep neural networks learn compositional data: The random hierarchy model. *Physical Review X*, 14(3):031001, 2024.

Ramon Ferrer I Cancho and Richard V Solé. The small world of human language. *Proceedings of the Royal Society of London. Series B: Biological Sciences*, 268(1482):2261–2265, 2001.

Aakanksha Chowdhery, Sharan Narang, Jacob Devlin, Maarten Bosma, and et al. Palm: Scaling language modeling with pathways. *arXiv preprint arXiv:2204.02311*, 2022. <https://arxiv.org/abs/2204.02311>.

Aaron Clauset, Cosma Rohilla Shalizi, and M. E. J. Newman. Power-law distributions in empirical data. *SIAM Review*, 51(4):661–703, 2009. doi: 10.1137/070710111. <https://doi.org/10.1137/070710111>.

Corinna Cortes, Lawrence D Jackel, Sara Solla, Vladimir Vapnik, and John Denker. Learning curves: Asymptotic values and rate of convergence. *Advances in neural information processing systems*, 6, 1993.

Nolan Dey, Gurpreet Gosal, Hemant Khachane, William Marshall, Ribhu Pathria, Marvin Tom, Joel Hestness, et al. Cerebras-gpt: Open compute-optimal language models trained on the cerebras wafer-scale cluster. *arXiv preprint arXiv:2304.03208*, 2023.

Ezra Edelman, Nikolaos Tsilivis, Benjamin Edelman, Eran Malach, and Surbhi Goel. The evolution of statistical induction heads: In-context learning markov chains. *Advances in neural information processing systems*, 37: 64273–64311, 2024.

Samir Yitzhak Gadre, Georgios Smyrnis, Vaishaal Shankar, Suchin Gururangan, Mitchell Wortsman, Rulin Shao, Jean Mercat, Alex Fang, Jeffrey Li, Sedrick Keh, Rui Xin, Marianna Nezhurina, Igor Vasiljevic, Jenia Jitsev, Luca Soldaini, Alexandros G. Dimakis, Gabriel Ilharco, Pang Wei Koh, Shuran Song, Thomas Kollar, Yair Carmon, Achal Dave, Reinhard Heckel, Niklas Muenennighoff, and Ludwig Schmidt. Language models scale reliably with over-training and on downstream tasks. In *Advances in Neural Information Processing Systems (NeurIPS)*, 2024. <https://arxiv.org/abs/2403.08540>.

Anthony Grattafiori and et al. The llama 3 herd of models. *arXiv preprint arXiv:2407.21783*, 2024. <https://arxiv.org/abs/2407.21783>.

Tom Henighan, Jared Kaplan, Mor Katz, Mark Chen, Christopher Hesse, Jacob Jackson, Heewoo Jun, Tom B Brown, Prafulla Dhariwal, Scott Gray, et al. Scaling laws for autoregressive generative modeling. *arXiv preprint arXiv:2010.14701*, 2020.

Joel Hestness, Sharan Narang, Newsha Ardalani, Gregory Diamos, Heewoo Jun, Hassan Kianinejad, Md Mostafa Ali Patwary, Yang Yang, and Yanqi Zhou. Deep learning scaling is predictable, empirically. *arXiv preprint arXiv:1712.00409*, 2017.

Jordan Hoffmann, Sebastian Borgeaud, Arthur Mensch, Elena Buchatskaya, Trevor Cai, Eliza Rutherford, Diego de Las Casas, Lisa Anne Hendricks, Johannes Welbl, Aidan Clark, et al. Training compute-optimal large language models. *arXiv preprint arXiv:2203.15556*, 2022.

Marcus Hutter. Learning curve theory, 2021. <https://arxiv.org/abs/2102.04074>.

A. Q. Jiang and et al. Mixtral of experts. *arXiv preprint arXiv:2401.04088*, 2024. <https://arxiv.org/abs/2401.04088>.

Daniel Jurafsky and James H. Martin. *Speech and Language Processing*. Prentice Hall, Upper Saddle River, NJ, 2 edition, 2009. ISBN 978-0131873216.

Dayal Singh Kalra. nanogpt-mup, 2025. <https://github.com/dayal-kalra/nanoGPT-mup>. commit 1e9b690bf91377f3cb2d4c9b4033d849c3303f5d.

Feiyang Kang, Newsha Ardalani, Michael Kuchnik, Youssef Emad, Mostafa Elhoushi, Shubhabrata Sengupta, Shang-Wen Li, Ramya Raghavendra, Ruoxi Jia, and Carole-Jean Wu. Demystifying synthetic data in llm pre-training: A systematic study of scaling laws, benefits, and pitfalls, 2025. <https://arxiv.org/abs/2510.01631>.

Jared Kaplan, Sam McCandlish, Tom Henighan, Tom B Brown, Benjamin Chess, Rewon Child, Scott Gray, Alec Radford, Jeffrey Wu, and Dario Amodei. Scaling laws for neural language models. *arXiv preprint arXiv:2001.08361*, 2020.

Mikail Khona, Maya Okawa, Jan Hula, Rahul Ramesh, Kento Nishi, Robert Dick, Ekdeep Singh Lubana, and Hidenori Tanaka. Towards an understanding of stepwise inference in transformers: A synthetic graph navigation model, 2024. <https://arxiv.org/abs/2402.07757>.

Margaret Li, Sneha Kudugunta, and Luke Zettlemoyer. (mis) fitting scaling laws: A survey of scaling law fitting techniques in deep learning. In *The Thirteenth International Conference on Learning Representations*, 2024.

Licong Lin, Jingfeng Wu, Sham M. Kakade, Peter L. Bartlett, and Jason D. Lee. Scaling laws in linear regression: Compute, parameters, and data. In *Advances in Neural Information Processing Systems (NeurIPS)*, 2024. <https://neurips.cc/virtual/2024/poster/95321>.

An Liu and et al. Deepseek-v2: A strong, economical, and efficient mixture-of-experts language model. *arXiv preprint arXiv:2405.04434*, 2024. <https://arxiv.org/abs/2405.04434>.

Yizhou Liu, Ziming Liu, and Jeff Gore. Superposition yields robust neural scaling. *arXiv preprint arXiv:2505.10465*, 2025.

Ashok Vardhan Makkula, Marco Bondaschi, Adway Girish, Alliot Nagle, Martin Jaggi, Hyeji Kim, and Michael Gastpar. Attention with markov: A curious case of single-layer transformers. In *The Thirteenth International Conference on Learning Representations*, 2025.

Alexander Maloney, Daniel A Roberts, and James Sully. A solvable model of neural scaling laws. *arXiv preprint arXiv:2210.16859*, 2022.

Eric J. Michaud, Ziming Liu, Uzay Girit, and Max Tegmark. The quantization model of neural scaling, 2024. <https://arxiv.org/abs/2303.13506>.

Niklas Muennighoff, Alexander M. Rush, Boaz Barak, Teven Le Scao, Aleksandra Piktus, Nouamane Tazi, Sampo Pyysalo, Thomas Wolf, and Colin Raffel. Scaling data-constrained language models. In *Advances in Neural Information Processing Systems (NeurIPS)*, 2023. <https://arxiv.org/abs/2305.16264>.

Elliot Paquette, Courtney Paquette, Lechao Xiao, and Jeffrey Pennington. 4+3 phases of compute-optimal neural scaling laws. In *Advances in Neural Information Processing Systems (NeurIPS)*, 2024. https://proceedings.neurips.cc/paper_files/paper/2024/hash/1dccfc3ee01871d05e33457c61037d59-Abstract-Conference.html.

Tim Pearce and Jinyeop Song. Reconciling kaplan and chinchilla scaling laws. *arXiv preprint arXiv:2406.12907*, 2024.

Guilherme Penedo, Hynek Kydlíček, Anton Lozhkov, Margaret Mitchell, Colin A Raffel, Leandro Von Werra, Thomas Wolf, et al. The fineweb datasets: Decanting the web for the finest text data at scale. *Advances in Neural Information Processing Systems*, 37:30811–30849, 2024.

Bryan Perozzi, Rami Al-Rfou, and Steven Skiena. Deepwalk: online learning of social representations. In *Proceedings of the 20th ACM SIGKDD international conference on Knowledge discovery and data mining*, KDD ’14, page 701–710. ACM, August 2014. doi: 10.1145/2623330.2623732. <http://dx.doi.org/10.1145/2623330.2623732>.

Steven T Piantadosi. Zipf’s word frequency law in natural language: A critical review and future directions. *Psychonomic bulletin & review*, 21(5):1112–1130, 2014.

Tomer Porian, Mitchell Wortsman, Jenia Jitsev, Ludwig Schmidt, and Yair Carmon. Resolving discrepancies in compute-optimal scaling of language models. *Advances in Neural Information Processing Systems*, 37:100535–100570, 2024.

Ofir Press and Lior Wolf. Using the output embedding to improve language models. *EACL 2017*, page 157, 2017.

Alec Radford, Jeffrey Wu, Rewon Child, David Luan, Dario Amodei, Ilya Sutskever, et al. Language models are unsupervised multitask learners. *OpenAI blog*, 1(8):9, 2019.

Yunwei Ren, Eshaan Nichani, Denny Wu, and Jason D Lee. Emergence and scaling laws in sgd learning of shallow neural networks. *arXiv preprint arXiv:2504.19983*, 2025.

Daniel L Ruderman. The statistics of natural images. *Network: computation in neural systems*, 5(4):517, 1994.

Utkarsh Sharma and Jared Kaplan. Scaling laws from the data manifold dimension. *Journal of Machine Learning Research*, 23(9):1–34, 2022.

Wei Shi and Yuan Cao. Towards understanding transformers in learning random walks. *arXiv preprint arXiv:2511.23239*, 2025.

Jinyeop Song, Ziming Liu, Max Tegmark, and Jeff Gore. A resource model for neural scaling law, 2024. <https://arxiv.org/abs/2402.05164>.

Stefano Spigler, Mario Geiger, and Matthieu Wyart. Asymptotic learning curves of kernel methods: empirical data versus teacher-student paradigm. *Journal of Statistical Mechanics: Theory and Experiment*, 2020(12):124001, December 2020. ISSN 1742-5468. doi: 10.1088/1742-5468/abc61d. <http://dx.doi.org/10.1088/1742-5468/abc61d>.

Richard Sutton. The bitter lesson. *Incomplete Ideas (blog)*, 13(1):38, 2019.

Changxin Tian, Kunlong Chen, Jia Liu, Ziqi Liu, Zhiqiang Zhang, and Jun Zhou. Towards greater leverage: Scaling laws for efficient mixture-of-experts language models. *arXiv preprint arXiv:2507.17702*, 2025. <https://arxiv.org/abs/2507.17702>.

Ashish Vaswani, Noam Shazeer, Niki Parmar, Jakob Uszkoreit, Llion Jones, Aidan N Gomez, Łukasz Kaiser, and Illia Polosukhin. Attention is all you need. *Advances in neural information processing systems*, 30, 2017.

An Yang and et al. Qwen2 technical report. *arXiv preprint arXiv:2407.10671*, 2024. <https://arxiv.org/abs/2407.10671>.

An Yang and et al. Qwen2.5 technical report. *arXiv preprint arXiv:2412.15115*, 2025. <https://arxiv.org/abs/2412.15115>.

Greg Yang and Edward J Hu. Tensor programs iv: Feature learning in infinite-width neural networks. In *International Conference on Machine Learning*, pages 11727–11737. PMLR, 2021.

Ge Zhang, Scott Qu, Jiaheng Liu, Chenchen Zhang, Chenghua Lin, Chou Leuang Yu, Danny Pan, Esther Cheng, Jie Liu, Qunshu Lin, et al. Map-neo: Highly capable and transparent bilingual large language model series. *arXiv preprint arXiv:2405.19327*, 2024.